Dynamic Weight Estimation of Non-Singulated Objects

by

Ayeda Sayeed

A thesis
presented to the University of Waterloo
in fulfillment of the
thesis requirement for the degree of
Master of Applied Science
in
Mechanical and Mechatronics Engineering

Waterloo, Ontario, Canada, 2018

AUTHOR'S DECLARATION

I hereby declare that I am the sole author of this thesis. This is a true copy of the thesis, including any required final revisions, as accepted by my examiners.

I understand that my thesis may be made electronically available to the public.

Abstract

Weight estimation is a common practice throughout many industries, though it typically requires that the objects to be weighed remain motionless. More often than not, it is beneficial to allow objects to move freely through a process, so that time is not lost in stopping and rerouting the object to a weight sensor. This is the basis for achieving dynamic weighing, where the object to be measured continues to have motion relative to the weighing sensor. Typically, this has been achieved with signal processing techniques that produce favourable results with singular objects. The challenge is when multiple objects are grouped and moving together; that is, they are non-singulated and cannot be weighed separately. This work reports the development of an In-Motion Weight Sensor array, which is a new dynamic weighing system with a new real-time signal processing method for estimating the weight of multiple, non-singulated objects. The array system employs a recursive least squares estimation algorithm to combine weight sensor data and the locations of boxes that are travelling through the array to attribute fractions of a box's load to the appropriate individual sensors. To demonstrate the performance of the proposed system, a full-scale experimental setup has been built and tested. Through statistical analysis of the weight estimates of a variety of groups of objects, it is shown that the system can produce results within 10% measurement error for the majority of non-singulated cases. It is most effective for non-rigid boxes that also fall within the mid-range for package size and weight, around 0.05m^2 and 1-3kg, respectively. Changes to the mechanical design can vastly improve performance accuracy and precision, and recommendations for these alterations are given in the conclusion.

Acknowledgements

The body of this thesis deals with a project that consists of a variety of different parts and subsystems. Similarly, its realization was only made possible with the contribution of a variety of people who have touched certain parts of the project. First, thank you to Bilal Maassarani, my predecessor in this continuing project, for the establishment of its framework and pioneering the way. Thank you to Mingu Kwon, with whom I never had the opportunity to meet, for the initial design of the In-Motion Weight Sensor array prototype. Thank you to Dahwan Kim, a co-op student with whom I worked closely to build, wire and validate the system prototype. Thank you to Meng Xi Zhu, of Tricolops Tcchnology, for his technical expertise and troubleshooting support in the area of integrating the dimensioning camera into the system. Thank you to Purolator Inc. for the collaboration opportunity and the support, and especially to Theo Pribytkov for his insight of research and development in the business world. Finally, a raucous and immeasurable thank you to my supervisor, Professor Soo Jeon, for his unlimited guidance and vision in the completion of this work.

Table of Contents

List of Figures

List of Tables

List of Abbreviations

AC/DC	Alternating Current to Direct Current
ADC	Analog to Digital Converter
ANFIS	Adaptive Neuro-Fuzzy Inference System
CAD	Computer Aided Design
CAN	Controlled Area Network
COM	Centre of Mass
EMFR	Electromagnetic Force Restoration
FIR	Finite Impulse Response
FPGA	Field Programmable Gate Array
IDE	Integrated Development Environment
IIR	Infinite Impulse Response
IMWS	In-Motion Weight Sensor
LAN	Local Area Network
LPF	Low Pass Filter
LSE	Least Squares Estimation
NI	National Instruments, Inc.
PC	Personal Computer
PWM	Pulse Width Modulation

RLS	Recursive Least Squares
RLSE	Recursive Least Squares Estimation
TCP/IP	Transmission Control Protocol/Internet Protocol
USB	Universal Serial Bus

This page intentionally left blank

Chapter 1
Introduction

Weight is one of the essential parameters to measure in many industrial applications, in particular in logistics and material handling. In mass production and distribution processes, the weight of an item often needs to be measured fast and accurately while items are moving in bulk on conveyors. The practice of weighing for such cases is referred to as *dynamic weighing* which means that the material being weighed is in net motion relative to the weighing machine [1].

Dynamic weighing is a key issue in some industry sectors. For example, in courier businesses, the transportation cost (for both air and ground) is determined by the gross weight as well as the total volume of loaded packages, so the correct knowledge of weight directly impacts their revenue. However, since packages are constantly moving on conveyors in a large quantity, it is not easy to identify the weight of individual packages. Unlike many other instruments employed in mass flow systems with conveyors (e.g. the laser dimensioners to gauge the volume of an item or cameras for tracking and sorting), measuring weight requires direct contact between the instrument and the target to be measured. More importantly, measuring weight essentially requires *singulation* of objects, i.e. each item must be separated from others so that it can be loaded, individually on a short section of the conveyor supported by a scale. Such a scale integrated with a conveyor belt is called the checkweigher [2] and it is widely used in industry for dynamic weighing.

The checkweigher may work very well if the items can be singulated. However, in practice, the checkweigher can rarely be used for mass flow conveyor lines where items are continually flowing through in bulk. This is because the singulation of items will cause the checkweigher to quickly become a bottleneck of the flow as each item in the queue is automatically stopped and rerouted, or manually loaded onto the checkweigher. See Figure 1.1 for some examples of randomly-oriented and non-singulated packages moving on a conveyor in bulk. Because of this reason, courier companies have been largely missing out (or simply relying on values self-declared by the client for) correct weight information, especially for corporate customers who place a large shipping order on a daily basis [3]. Consequently, the volume (or the dimension) of a package has been the only physical parameter that is usually measured in-situ for such mass flow systems.

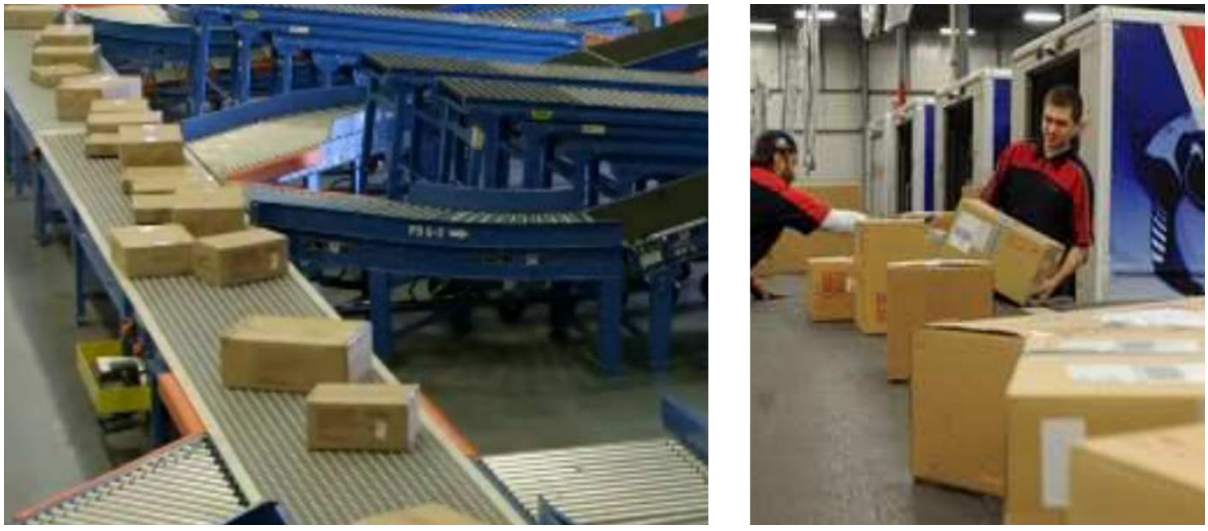

Figure 1.1: Randomly-oriented packages moving on a conveyor in a non-singulated manner (courtesy of Purolator Inc.)

1.1 Motivation

The work in this thesis is the outcome of a research collaboration with Purolator Inc. Purolator is a major freight and parcels solutions provider in Canada. As a courier company, Purolator's operation relies on distribution centers in major cities of the country. Distribution centres sort parcels by using an integrated belt conveyor system, the main operations of which include path diversions, pushers, and speed variations to assist in the automation of sorting. Additional sensors such as dimensioners, barcode scanners, cameras and check-weighers are also used along with the conveyor systems to differentiate the parcels according to size, destination, weight, etc. If the customer declares an incorrect weight, the company may lose money on the sale of their service. An underestimated weight may also disturb the logistics process by attempting to accommodate parcels into the delivery vehicle in excess of the maximum limit.

In the collaboration with Purolator as an industry partner, the goal of this research is to achieve accurate and efficient weight measurements while parcels are moving in a random, non-singulated manner. In this way, Purolator can avoid the bottleneck in sorting and distribution facilities, and thus can make correct pricing. While finding the solution to this problem can be a standalone project, it also opens avenues to investigate the application of engineering controls methods that are typically used in what are considered broader and more advanced fields.

The general problem to be solved is the concept of dynamic weighing: determining the weight of multiple objects as they are moving. This has been addressed in industry with generally slow and

inefficient methods, usually requiring singulation, that are discussed in Section 1.2. While these methods can provide inspiration for conceptual designs of a solution catered to the dynamic weighing of parcels, they typically require manual set-up or are better equipped to handle continuous flow of usually granular product. From the standpoint of technological advancement, a fully automated process for dynamic weighing of non-singulated product would make a larger contribution to the industry of parcel distribution.

1.2 Background of Dynamic Weighing Methods

The Weighing and Force Measurement Panel of the Institute of Measurement and Control performed a study of all dynamic weighing methods currently available [1]. These methods include any system where the product can be in motion relative to the weighing machine. For example, selective combinational weighers are systems that employ multiple weighing heads to statically weigh discrete portions of product and then calculate the best combination of the weighed portions to fulfil a target weight to be packaged. This type of system eliminates the need for a labourer to make the decision of which portions or pieces of product to fill the package with, thus automating and speeding up the process. While this is not specifically applicable to the solution required for parcel distribution, it provides an introduction into the concept of employing multiple weighing units for a single purpose, as well as singulation of product and a sequence of discrete steps required in the weighing process.

Many of the methods outlined in [1] are used for distribution of food or some other particulate products that are usually in some form of continuous flow. They also have the common goal of filling a target weight (for packaging) and do not singulate individual articles of product to record their weights. Finally, these systems tend to use controlled vibration in belt conveyors to separate product when needed, which is not desirable in the parcel industry as the strong vibration required to shift large and heavy parcels could damage the customers' goods. The document largely covers these types of weighers, but also includes in-motion systems that include discrete mass weighing systems that prove useful to parcel distribution and are described in this section.

One of the applicable in-motion methods is the weighbridge. A weighbridge is a system that utilizes weigh platforms to measure individual wheel or axle loads as a vehicle traverses the platforms. Weighbridges are used with vehicles on a road as well as locomotives on a rail. The final and most applicable method is catch weighing. Some specific weighers for dynamic weighing are reviewed in more detail in the following subsections.

1.2.1 Catch Weighing

Catch weighing methods will weigh individual items and use the measurement to either categorize the item (Check Weighers) or describe the item (Catch Weighers). Check weighing devices usually determine if the measured item falls with acceptable limits of a batch category and can reject items that do not comply. General catch weighers are typically used to determine the total price of the measured item based on a unit cost. Both types of weighers will typically use a belt system to transport the items, and this belt is supported by weight sensing devices.

Figure 1.2: A catchweighing technology [4] © Pico Automation

The performance of both types of catch weighers depends heavily on the system throughput, as both methods are making a calculated decision based on the weight measurement instead of simply providing the weight. The factors affecting this performance include: measurement sensor type and the inherent measurement errors of each component of the system, the overall mechanical design and resulting vibrations, speed of operation, the item weight, and the nature of the product in the item (e.g. movement of contained liquids).

1.2.2 Vehicle Weighbridges

The conventional weighbridge is a dynamic weighing device used to weigh single axles of vehicles, which are loaded onto the platform. **Error! Reference source not found.** shows the resulting relationship between accuracy class for axle load (in increasing error) and accuracy class for total measured vehicle

mass. The accuracy of the conventional method is affected by the speed of travel of the vehicle, forward versus reverse operation, braking versus acceleration operation, the topography of the road before and after the weighbridge, and any deficiencies in the road surface. Thus, conventional weighbridges provide the best accuracy when the vehicle is held stationary before the weighing procedure beings and does not perform as well for true in-motion processes.

Table 1.1: Relationship between measured accuracy for axle loads and measured accuracy for total vehicle mass [1, Tab. 5.2.1.4]

Accuracy class for axle load	Accuracy class for total vehicle mass (% of total vehicle mass)					
	0.2	0.5	1	2	5	10
A	✓	✓				
B	✓	✓	✓			
C		✓	✓	✓		
D			✓	✓	✓	
E				✓	✓	✓
F						✓

The foundation-less weighbridge employs weight-sensing pads on the road and can easily be modified for different configurations of vehicles. While the same factors as the conventional method affect the foundation-less method's accuracy, the foundation-less method performs well in both stop-and-go and in-motion processes, producing measurements within 2-3% of total vehicle weight.

Figure 1.3: Portable weighbridge [5] © 2013 Griffith Elder and Company Ltd

Rail weighbridges weigh the wheel, bogie, wagon and total train load. These weighbridges are also divided into conventional load cell and foundation-less methods, as well as portable methods that are typically used temporarily for purposes of checking safety compliance. The foundation-less methods are further divided into categories of in-track, active sleeper, and surface mount, referring to their orientation relative to the railway track. The number of wagons in the train affects the overall accuracy of the total measurement. For slow speeds (within 10km/h) an accuracy of 0.25% can be achieved for total train weight.

The concept of weighbridges can inspire the use of multiple discrete weight sensors, while the catch weighers provide a recommendation for the use of belt conveyors to continuously move items.

1.3 Related Work on Weight Estimation in Dynamic Weighing

Checkweighers are commonly used to determine the weight of objects while they are transported via conveyor belts, especially in the parcel distribution industry. The objects are routed towards a static (an isolated scale) or dynamic (a short section of conveyor belt that is supported by a scale) checkweigher, but not before being manually or automatically singulated so that only a single object at a time is loaded onto the checkweigher.

Mettler Toledo, a measurement solutions provider, offers a “mass flow” dimensioning technology that integrates and stores object ID, dimensions and weight, allowing for objects to continue to be measured without individual singulation [6]. However, the weight measurement may not provide the level of accuracy that is required by many industry clients.

Figure 1.4: The CSN210 MassFlow™ weighing and dimensioning technology by Mettler Toledo [6] © Mettler Toledo

The checkweigher's scale (weight sensor) is a load cell, which employs a Wheatstone-bridge circuit configuration to convert vertical displacement into an electrical signal. Even without supporting an additional belt conveyor, this kind of system is already susceptible to noise and non-linear transient behaviour, which deteriorates the system's accuracy and reliability. This, coupled with the logistical strain of rerouting objects to a checkweigher have made it an interesting system to analyze and improve.

The checkweigher problem has been analyzed in different angles, employing filters to reduce the noise from mechanical vibrations as well as dynamic models to attenuate disturbances during the transient stages of loading objects into the checkweigher. Notably, these solutions assume that the objects to be weighed are already singulated, and that only a single object is loaded onto the checkweigher at any given time. Nonetheless, these investigations offer an avenue for attenuating noise and disturbances as an attempt for achieving higher measurement accuracy and can be applied either in isolated cases where object singulation has already been achieved or in conjunction with other algorithms that can apportion one weight measurement to multiple objects.

In practices of dynamic weighing, singulation has been considered inevitable to determine the weight of individual items. Hence, research on dynamic weighing has mainly been focused on improving its accuracy when items move on a checkweigher one at a time [7]-[17]. This has been the case even for fluidic bulk materials (e.g. powders, granules or liquids) which are usually pre-packaged into individual batches (and thus singulated) before they are loaded for dynamic weighing [1].

The central problem in dynamic weighing is the oscillation in the measured weight signal. The oscillation may come from the mechanical vibration associated with moving parts and/or impact caused by loading and unloading of the item. The majority of studies including those listed above, therefore, have been focused on developing effective signal processing techniques to compensate for those unwanted oscillations. Approaches in the literature range from digital filtering techniques [10], [14]-[16] (often with time-varying coefficients) to more advanced model-based estimation techniques such as Kalman filtering [9], [11].

The references considered so far have mostly been used for strain-gauge-based load cells which are essentially a passive instrument in the sense that there is no active control over the transducer during the measurement process. Another type of load cells that are based on electromagnetic force restoration (EMFR) [17] can realize faster and more accurate weight measurement through realtime feedback control. Compared to strain-gauge load cells, the EMFR can be more suited for dynamic weighing because oscillations caused by dynamic weighing can actively be canceled through high speed feedback control of the electromagnetic force that is in balance with the weight. Because of this, many studies have been devoted to modeling and control for EMFR-based checkweighers [18]-[24]. An example of one such checkweigher is shown in Figure 1.5.

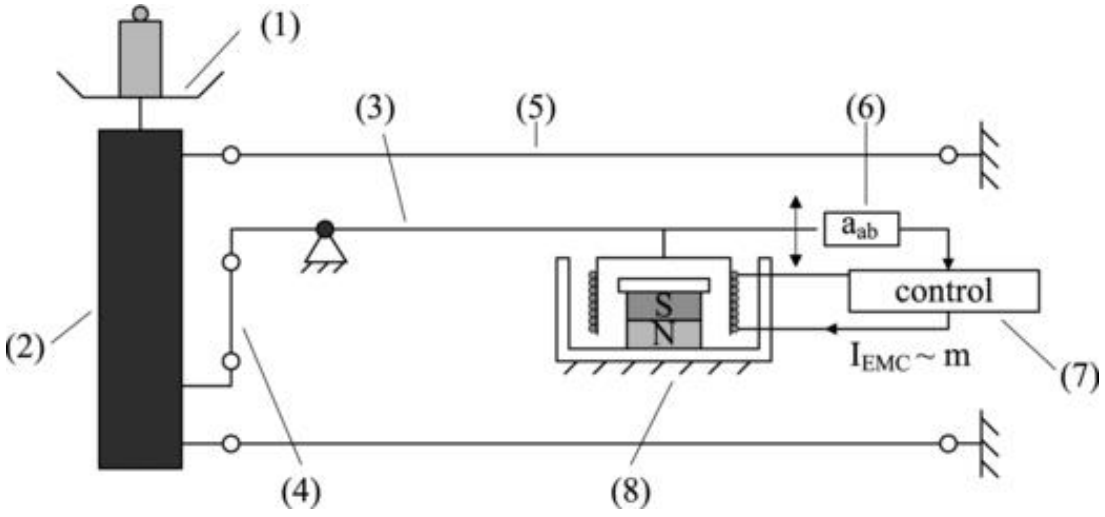

Figure 1.5: Basic operation of an EMFR weighing system. (1) weighing pan, (2) pan carrier, (3) conversion lever, (4) coupling element, (5) parallel beams, (6) optical position sensor, (7) control loop, (8) voice coil with permanent magnet [21, Figure 1]. © 2012 IOP Publishing Ltd.

1.3.1 Basic Filters

A basic low-pass filter typically attenuates most of the noise due to electrical noise (especially from the switching in the motor control for moving the belt) as well as that from mechanical vibrations. The response time of a low-pass filter must be sacrificed in order to achieve higher accuracy, and so what a low-pass filter fails to attenuate is the one-time transient behaviour from loading an object onto the checkweigher. A low-pass filter alone cannot be used to improve checkweigher performance. Instead, some more complex signal processing techniques must be used.

Ono et al attempted two different applications of the Kalman filter with varying success [11]. The first method assumed a linear model for the checkweigher, where the weight of the object was much smaller than the weight of the checkweigher scale. This linear system Kalman filter model can be used in real-time, however the linear model is not realistic, especially in the case of non-singulated objects. The second method assumed a non-linear model an used a truncated second-order Kalman filter, which allowed for a time-varying filter that unfortunately could not achieve real-time data processing.

1.3.2 Model of the load cell

Tariq, Balachandran and Song expanded on the typical model of the load cell and developed a series of checkweigher models to encompass the entire system, from the infeed conveyor all the way to the outfeed conveyor (which are located before and after the weighing unit, respectively) [26]. First, the typical mass-spring-damper model is used for the actual weighing sensor. They also introduce three forcing functions for describing different package types to be used with this model: type 1 for solid packages, and types 2 and 3 for loose medium packages. Furthermore, the package model accounts for horizontal and vertical disturbance forces, as well as a tilting effect due to horizontal disturbances that arise from speed differences between conveyor belts. Finally, the conveyor transport subsystem model involves the infeed (or outfeed) conveyor interacting with the weighing conveyor and includes motor dynamics, belt friction, and masses and dimensions of the supported conveyors.

1.3.3 Model-based parameter estimation

Halimic and Balachandran continued with the previously described models and applied a Kalman filter [27]. They found that this solution was effective for non-linearities in the system and when the low frequency noise to be attenuated falls within the useful bandwidth of the sensor signal.

1.3.4 Combinational Advanced Signal Processing with Model-based estimation

Yamazaki et al combined the dynamic model of the individual checkweigher (load cell with conveyor belt) with finite impulse response (FIR) filters to estimate the weights of each object in a discrete sequence [16]. The finite response of the filter is important here so that the loading input from the checkweigher can return to zero as quickly as the objects enter because the process conveyors in industry will be running at such high speeds that the checkweigher response needs to be able to match these speeds.

To maintain a discrete sequence, the distance between objects is always greater than the difference between the checkweigher length and the subsequent object length. In this way, the loading input of the subsequent object can be identified and isolated from the fully-supported input of the preceding object (or the preceding object is unloaded from the checkweigher before the subsequent object is fully-supported).

The FIR filter down-sampled the measurement data at rates up to 8 times slower than the measurement sampling, and was cascaded with a low-pass filter to attenuate noise due to quantizing the signal. The weight estimate of each object was determined from the maximum value evaluated from the final processed signal. While this method claimed that 0.7% measurement accuracy can be achieved, the experimental results show that objects with smaller masses tend to have the largest deviations. As expected, the FIR filter with the slowest sample time provided the smoothest results.

1.3.5 Electromagnetic Force Restoration

The fundamental operation of an EMFR weight sensor is described in [17] and [19] and involves the following major components: a weighing platform, a Roberval mechanism, an electromagnetic force actuator, an optical position sensor, and a controller, all shown in Figure 1.5. The object to be weighed is placed on the platform, which is coupled with the Roberval mechanism.

The double levers in the Roberval mechanism ensure that the tilting effects of the platform are also compensated. The double levers are joined in such a way that they must always hold a parallelogram shape. This allows the object to be placed anywhere on the platform, and the resulting parallelogram ensures that the vertical displacement is the same for any other placement location of the object.

It is this vertical displacement that is representative of the weight of the object, and so, through a combination of levers to achieve the desired scaling, an optical position sensor will detect when the force transferring lever's position has shifted from equilibrium. The displacement elicits a balancing response from the electromagnetic force actuator. The controller uses the position sensor in a feedback loop to

determine the electrical current required to apply to the electromagnetic to generate the force that maintains the equilibrium. The controller then uses this information to determine the weight of the object.

In addition to the position sensor, a temperature sensor can also be added into the loop to compensate the current loss, and further modification of the control loop can compensate for mechanical vibrations. This results in a highly accurate weight measurement system that can be coupled with a conveyor belt to achieve dynamic weighing.

1.3.6 Intelligent Systems

It is also possible to take advantage of fuzzy logic and neural networks by combining them to form an Adaptive Network based Fuzzy Inference System (ANFIS) to improve the accuracy and throughput rate of a checkweigher [28]. A fuzzy inference system learns from an input-output data set to tune the membership function parameters to be used in the fuzzy part of the overall system. In [28], Halimic et al propose a clustering algorithm to determine the initial number and shape of these membership functions.

1.4 Progress Made Before This Thesis

The problem of dynamic weighing that is specific to Purolator Inc. was first tackled by another graduate student at the University of Waterloo. Maassarani began the design of the prototype hardware and applied several post-processing solutions to validate the weight estimation of the system with a single object [29]. The major methods described in his dissertation involve a discrete time-variant low-pass filter, as prescribed by [15], and a model-based parameter estimation as outlined by [7], [11] , [26], [27], and [30].

1.4.1 Discrete Time-variant Low-pass Filter

Maassarani concluded that the preferred method is the discrete time-variant low-pass filter because it is developed independent of the system model, thus making it more robust to vibrations and noise, despite requiring extensive tuning of the cut-off frequency through experimentation. The filter is designed by cascading first-order IIR filters of the form:

$$\boldsymbol{y_i(n) + a_k(n) y_i(n-1) = b_k(n)[y_{i-1}(n) + y_{i-1}(n-1)]} \qquad (\mathbf{1.1})$$

where:

$i = [1, \dots, k]$ with k being the number of filters in cascade;

$n = [1, \dots, N]$ the time steps until the load begins to leave the weighing platform;

The output of the load cell in question is the input to the cascade and the estimated weight is the output at $y_k(N)$. The coefficients are calculated as functions of the time-variant cut-off frequency and sampling period.

The time-variant cut-off frequency decays exponentially to shorten the transient response. It begins at an initial value of f_0 and decreases to a limit of f_∞ at a rate of α and is calculated as:

$$f_c(n) = f_\infty + (f_0 - f_\infty)\lambda^{\frac{n-1}{\alpha(N-1)}} \tag{1.2}$$

where:

λ is arbitrarily small;

α is tuned through experimentation;

f_∞ is chosen based on the frequency analysis of the load cell response;

f_0 is optimized with a cost function for accuracy.

1.4.2 Model-based Estimation

Since load cells are designed like dual cantilever beams with one-dimensional displacement, we can model the weight that they measure using a mass-spring-damper model. Taking into consideration m_l, the weight detected by the load cell when it is empty, we have:

$$w(t)g = (w(t) + m_l)\ddot{\theta}(t) + c\dot{\theta}(t) + k\theta(t) \tag{1.3}$$

where:

$w(t)$ is the weight of the object, in kg;

g is the gravitational constant, 9.81 m/s;

m_l is the weight detected by the load cell when empty (i.e. without an object to be measured);

$\theta(t)$ is the displacement of the load, in m;

c is the linear damping coefficient, in kg/s;

k is the linear stiffness coefficient, in N/m.

Putting this into state space form and including the effects of stochastic mechanical disturbances and electrical measurement noise, the model yielded good results in simulation when compared to experimental verification. However, its simulation of the transient behavior of the load cell is not accurate enough to use the model for analysis other than the steady state period where the object is fully supported by the load cell. The model expects a more gradual ramp to steady state than what is shown in reality.

Thus, the transient response was ignored to develop the identification-based approach. Taking the last sample when the object is fully supported as the steady state value, the model can be represented as:

$$(M + m_l)\ddot{\theta}(t) + c\dot{\theta}(t) + k\theta(t) = Mgu(t) \tag{1.4}$$

where:

M is the time variant mass of the object (previously $w(t)$);

$u(t)$ can be the step function input, to represent the presence of an object on the load cell.

Non-zero initial conditions must be assumed since the load cell will attain a non-zero output during its transient response before the steady state period that we are observing. Taking the Laplace transform of the above equation and then further discretizing it (since the load cell output signal is processed through an ADC) yields:

$$\Theta(z) = \frac{Mg}{k}U(z)\frac{{b_1}^* z^{-1} + {b_2}^* z^{-2}}{1 + a_1 z^{-1} + a_2 z^{-2}} + \theta(0^+)\frac{1 + \alpha z^{-1}}{1 + a_1 z^{-1} + a_2 z^{-2}} \tag{1.5}$$

where:

a_1,a_2,${b_1}^*$,${b_2}^*$ are related to the sampling time T, damping ratio ζ, and natural frequency ω_n;

α is an expression that exists to relate a_1 and a_2 with the initial conditions $\theta(0^+)$ and $\dot{\theta}(0^+)$.

Eq. 1.5 can be compacted further with b_1 and b_2 as expressions of ${b_1}^*, {b_2}^*, \alpha$, and $\theta(0^+)$. After applying the final value theorem, and combining b_1 and b_2, the mass can be estimated as:

$$M = \frac{b}{1 + a_1 + a_2} \tag{1.6}$$

As the input is assumed to be a step function, its value is constant and so a difference equation can be used to represent the system parameters b, a_1, and a_2 which can then be estimated using the least squares method so that:

$$\hat{m}(N) = \frac{\hat{b}(N)}{1 + \hat{a}_1(N) + \hat{a}_2(N)} \tag{1.7}$$

is the final mass (or weight) estimate.

1.4.3 Results

Both methods are useful in situations where only one object is passing over a single load cell. Maassarani compared the results of the time-variant low-pass filter with that of the model-based estimation for experiments consisting of a single package traveling over a single load cell. It was found that the time-variant low-pass filter had the best performance in terms of minimizing measurement error. The model-based estimation method is susceptible to noise, which can be addressed by cascading a low-pass filter with the system. However, low-pass filters introduce a tradeoff between accuracy and settling time, thus Maassarani concludes that the time-variant low-pass filter is the preferred method for estimating the weight of a single object [29].

1.5 Contribution of This Thesis

In a recent patent [3], Purolator has shown that previous technologies that incorporate dimensioning with weight measurement of non-singulated objects failed to properly dimension objects outside of the focal center of the dimensioning system and also failed to assign individual and accurate weights to single objects. The patent describes a technology that can determine the weight of an item, even when included amongst a group of items, which is described as a mass flow environment, regardless of their arrangement or orientation, and also attribute dimensions to these individual items so that all of this data is stored in a computer in order to generate revenue on item weights that must be adjusted. Thus, the specifications for this project were formulated.

This thesis summarizes the progress that has been made on the system design and the algorithm development for the In-Motion Weight Sensor (IMWS) array. The IMWS array realizes the full-scale system that can accomplish the identification of individual packages moving on a conveyor in a non-singulated way, in contrast to traditional methods that simply measure solitary, singulated packages. The developed algorithm uses an overhead dimensioning camera to its advantage to identify exact locations of the packages, and also estimates the fraction of the package's surface area that is supported by individual load cells. This area fraction is assumed to be correlated to the fraction of the package's load that is supported by the cell, and is used to apportion the weight measurement from a cell to the multiple packages that it supports. An implementation of the recursive least squares estimation method combines the multiple area fractions with the array of weight measurements to estimate the weight of each package in a group over the period that they travel over the shared surface of the system. A series of experiments

were conducted with test packages of known weights in a variety of orientations and combinations to produce good statistical results. This statistical analysis demonstrates the system's ability to estimate the weight of the majority of non-singulated rectangular objects within 10% measurement error, and also indicates the ideal package size and weight range that produces the most accurate results. Recommended changes to the design of the IMWS system are given at the end of this thesis to improve the overall estimation accuracy, as well as other algorithms and avenues for increased functionality and performance.

Chapter 2
Design and Fabrication of the Prototype

The scope of project with Purolator included to design and build a functioning full-scale prototype for the solution of the singulated and dynamic weighing of packages. Specifically, the design requirements include [3]:

- Integration of machine vision to determine when an item is supported by two or more load cells, and allocate the load cell data to the item
- Ability to control speed of conveyors
- Ability to determine the locations and orientations of items relative to the system space in real-time
- Assigning a unique identification tag associated with each item and weight
- To be able to alert the user when the measured weight differs from predetermined weight data associated with the identification tag (i.e. consumer-declared weight)

This chapter covers the conceptualization and design of the final prototype of an In-Motion Weight-Sensor (IMWS) array that was developed to meet the design requirements listed above. Although the prototype has been designed with industry standard in mind and to comply with the requirements outlined in [3], it is expected to be modified in the future for adaptability into industry operations. Nevertheless, it currently serves as proof-of-concept device for experimentation and implementation of main research ideas put forward in this thesis.

2.1 Mechanical Design

As mentioned earlier, the major issue with dynamically measuring the weight of multiple objects is the singulation of the individual objects. Therefore, it was imperative to find a concept that promotes singulation of the packages within its structure. A grid concept has been chosen as the most viable system structure to this end.

By utilizing an array (or grid) of weight measurement cells (or modules), the location of parcels can be narrowed down to a collection of cells, and their mass information can be singulated even before the

parcels are physically singulated. Each parcel can be supported by multiple cells. Likewise, each cell may support multiple packages. This array of weighing cells provides mass data to be collected for each parcel at different points in the array as it moves through it. This is how the dynamic weighing is achieved, and also provides more mass information for a moving average, etc. However, if multiple packages are weighed on the same cells, physical singulation may be required. Thus, in this prototype, each cell also consists of an individually controlled belt conveyor that can accelerate or slow down independently from its neighbours in order to rotate a parcel or to create a space between a parcel and the one following directly behind it.

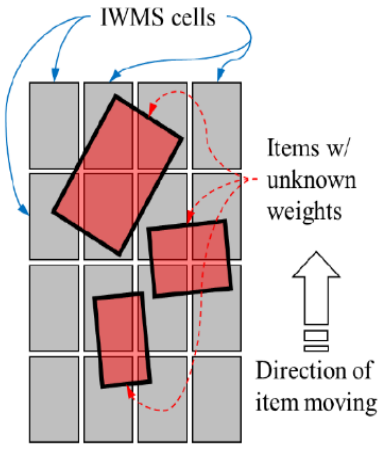

Figure 2.1: Grid concept

2.1.1 Conveyor Design

A conveyor belt module is mounted to each weight measurement cell in the IMWS array. To achieve independent control of each cell for parcel singulation, each conveyor module required an independently-controlled motor that is housed within the module itself to reduce its bulk and the overall footprint of the prototype. This design is shown in Figure 2.2 and Figure 2.3. With the motor positioned in the center of the conveyor housing, the shaft extends out enough to accommodate a timing belt that controls a driving pulley. The driving pulley rotates a large roller to actuate the belt, and the driven roller rotates with the belt to reduce friction losses.

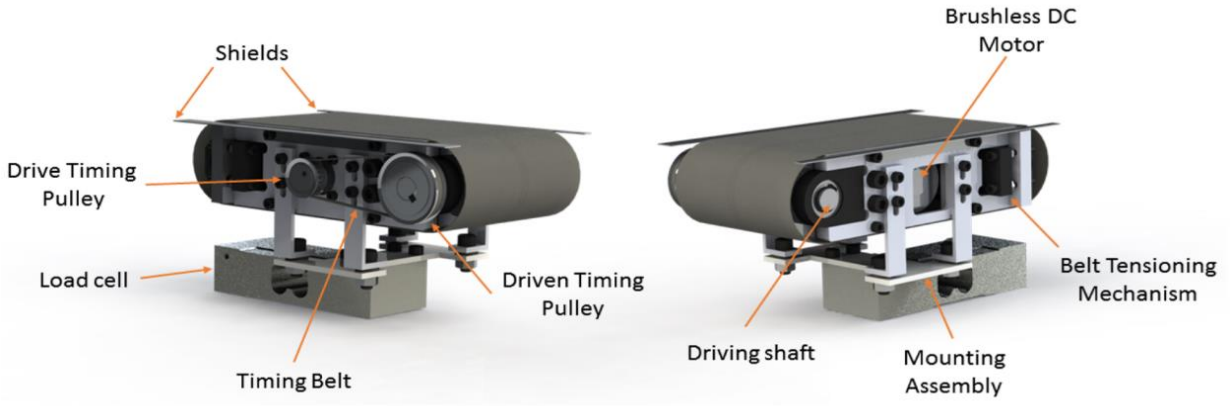

Figure 2.2: CAD rendering of conveyor model [29]

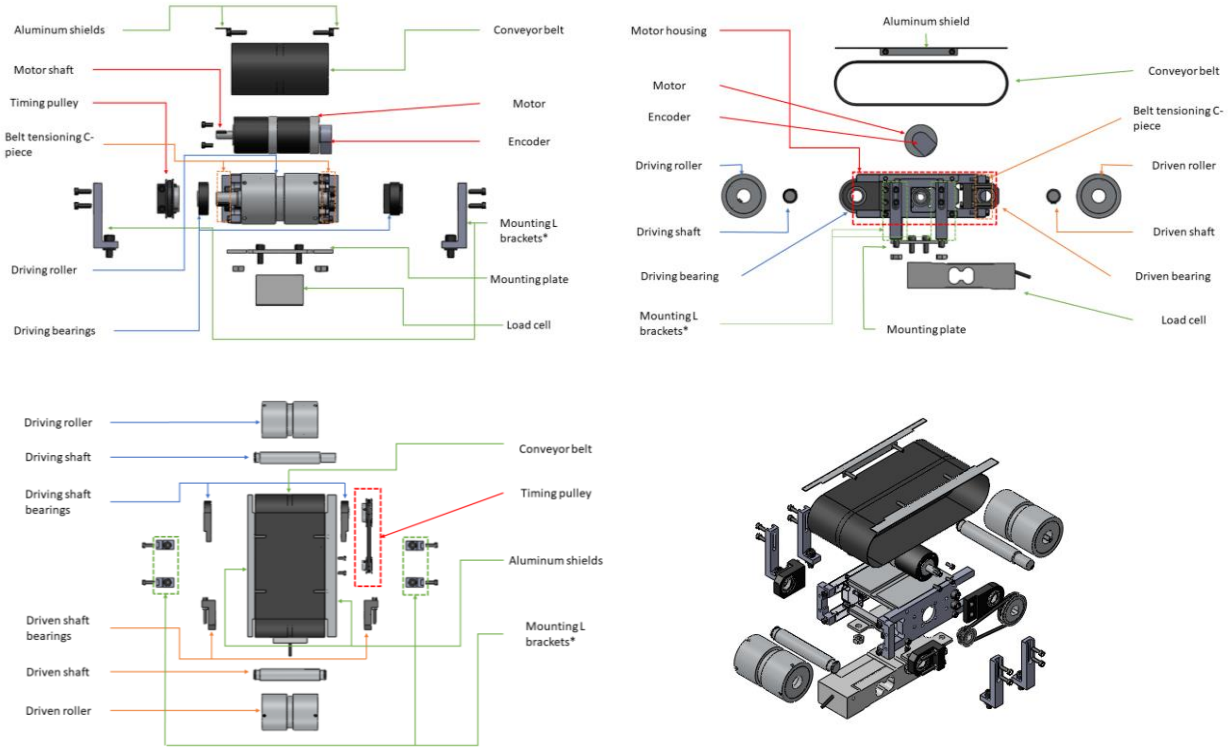

Figure 2.3: Exploded view of the CAD model of the conveyor unit to show individual parts

The mounting L brackets shown in the above Figure 2.3 have changed slightly between the design and fabrication stage. Instead of two separate L brackets on either side, each pair is joined in the middle as a single piece, so that there are now two U-faced L-brackets, one for each side of the conveyor module.

2.1.2 Belt Tensioning Mechanism

Applying the correct amount of tension to the conveyor belt posed another major challenge to the module design. It was necessary to be able to assemble each module by hand, and the belt must be fitted over the module after the conveyor has been fully assembled (but before the mounting brackets are affixed to the module). So the belt must be looser than the assembled housing in order to fit it on. However, the belt is moved by tension between it and the surface of the rollers, so the housing must grow to fit the belt after it has been fitted. Thus the belt-tensioning mechanism was developed.

To extend the length of the conveyor module, the driven shaft and roller subassembly is designed to move in the longitudinal direction, whereas the driving roller subassembly remains fixed as it is mated to the motor via the timing pulley. The bearings for the driven roller are mounted to the module through the spine of a protruding C-piece. The C-piece protrudes in the lateral direction from the rest of the housing, allowing for screws to insert into the C-piece along the longitudinal axis of the module, extending past the C-piece when tightened far enough. The bearing housing consists of a thick L base, as shown below in Figure 2.4.

Figure 2.4: Bearing for driven roller

The bearing and C-piece are oriented so that the C-piece is in between the bearing base and the axis of the bearing shaft, where the shaft is situated furthest from the center of the module relative to the C-piece and bearing base. The holes in the bearings and the C-piece are threaded for the screws. On the other hand, the nuts are screwed on between the bearing and the C-piece, instead of after the C-pieces, so that

tightening the screws within the nut draws the base towards the C-piece. The orientations of all of these components are shown in Figure 2.5.

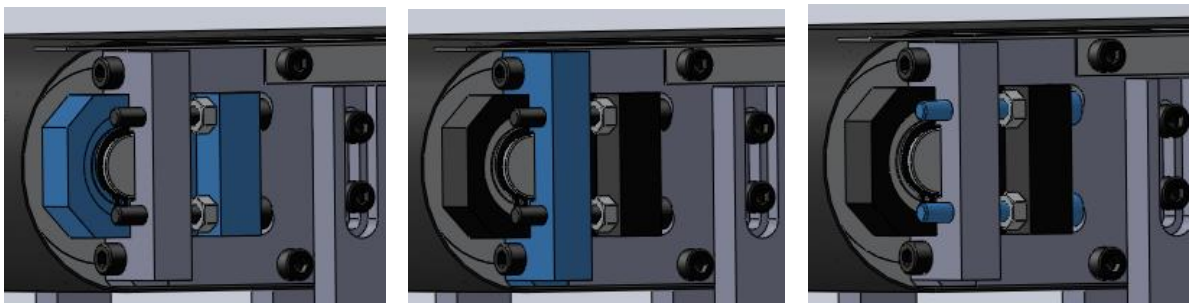

Figure 2.5: Components used for tensioning the belt, highlighted in blue

When the conveyor is initially assembled, the maximum allowable space is left between the nut and the bearing base so that the roller is “pulled in”; that is, the conveyor is at its shortest possible length. The screws are then turned, pulling the bearing base closer to the C-piece, thus “pushing out” the roller and extending the overall conveyor length. In this way, the conveyor module grows to fit the belt. The nuts are tightened to keep the bearings' positions when the desired length and desired belt tension is achieved.

2.1.3 Conveyor-Load Cell Module Prototype

The completed module components are machined from aluminum and assembled by hand, utilizing non-permanent mating techniques such as interference fits and nuts and bolts. The motor is housed within the module, with wire connections hanging out to connect to the motor driver. The belt is a (material) with an inner guiding strip that follows an indent in the top of the module to keep the belt centered. This entire conveyor is mounted to the weighing surface of a load cell via two slotted L-brackets and a mounting plate. The slots in the L-brackets allow for height adjustment of the whole unit. Thin aluminum shields overhang from the top of the long edges of the conveyor to protect the moving parts of the conveyor and the travelling objects from each other. The assembled conveyor-load cell module is shown in Figure 2.6. It has a footprint of 190 x 308mm.

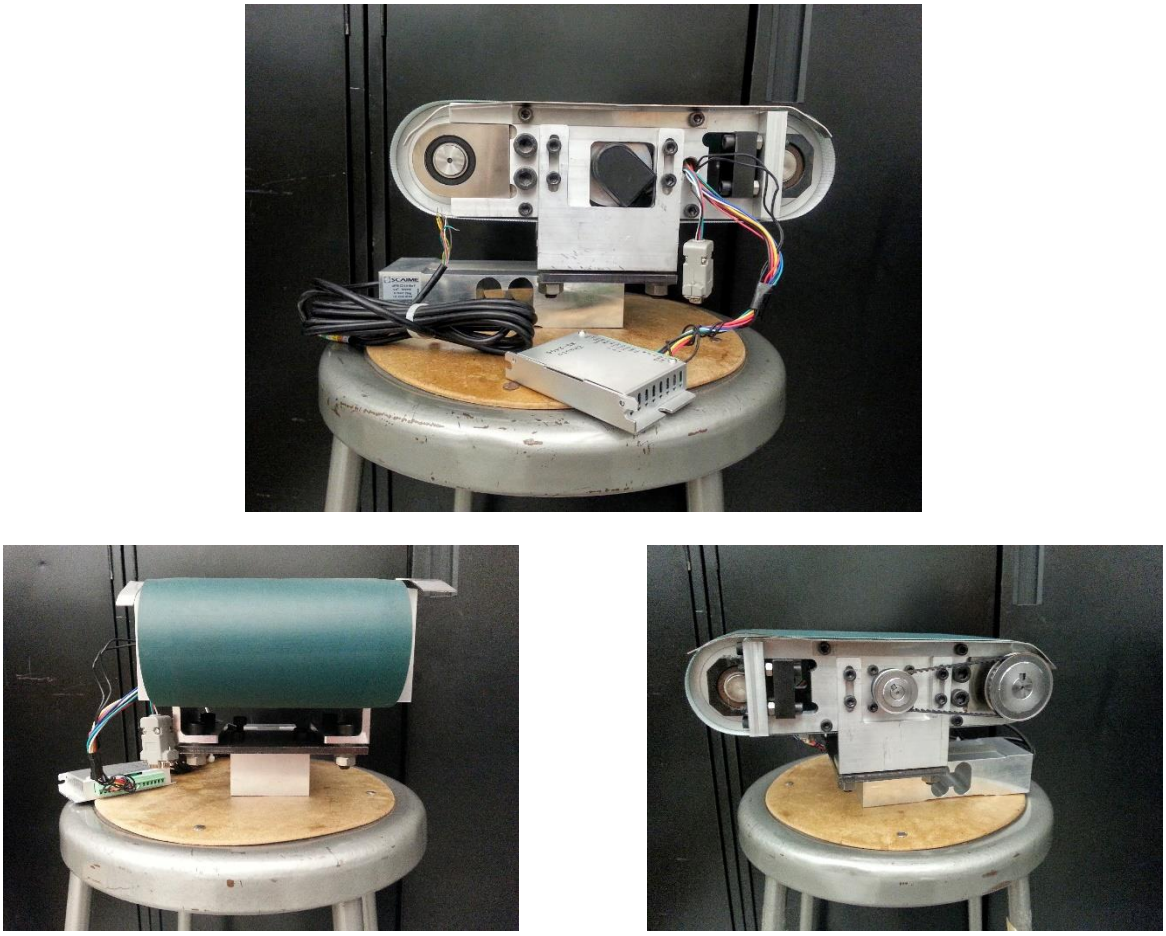

Figure 2.6: Assembled conveyor-load cell module

2.2 Electrical Design

The electrical design of the prototype is relatively straightforward and utilizes many commercial solutions to ensure robustness. Load cells are used as the basic weight sensors in each module. The manufacturer of the load cell in the IMWS array also provides a signal amplifier and transmitter unit that converts the raw voltage from the load cells to readable values to be transmitted on a CAN network. The unit also provides local conditioning, calibration, and filtering. The motors in each conveyor module are controlled by a single motor driver. An intermediate data acquisition controller caters to the load cells and motors, while another PC consolidates the data from an overhead infrared dimensioning camera and the intermediate controller. This camera provides positional data for every rectangular object detected in each frame, useful to associating specific load cell measurements to the detected objects.

2.2.1 SCAIME Load Cell System

A load cell was chosen as the base weight sensor, as it was the most compact and economical option with the appropriate surface area for supporting a conveyor module. The actual weight measurement unit chosen for the IMWS array is a load cell manufactured by the French company SCAIME, who provides weight and sensing solutions for industry. The load cell model used in the design is the AP 75, an aluminum, single-point load cell. They can support up to 75kg in measurement each and allow for a weighing platform to be mounted directly to the load cell itself. This is how the mounting brackets are screwed directly into the load cell.

Each load cell comes with a signal amplifier, called the eNod4-c transmitter (henceforth known as an "eNod", for brevity). These transmitters are wired to one load cell only, and convert the raw voltage from the load cells to a readable value to be transmitted through CAN, Profibus, or USB. The transmitters also provide local conditioning, calibration, and filtering. Each load cell can be calibrated according to its local conditions (e.g. gravitational acceleration constant changes slightly with geopositional coordinates), a zero offset can be set (for initial payloads, in this case the conveyor units), scaling and taring conditions can be set, and local signal filters can also be tuned. These calibration settings can be accessed with a PC via USB so that each load cell can be calibrated individually. In this prototype, we use second-order low-pass filters with a cut-off frequency of 4Hz in conjunction with a self-adaptive filter, both internal to the eNods. The data networks allow all eNods to dump their information onto the network to be read by a master controller.

2.2.2 Motor and Power Electronics

The motor system in each module consists of a motor and motor driver, both of which were purchased from Chinese manufacturers, and fit the torque and power ratings required of the IMWS array. The assembled conveyor can achieve speeds of up to 370rpm, resulting in a belt speed of 0.78m/s. The motor drivers are powered by AC/DC converters, that step down the 115VAC wall power to the 36V required of the motors.

2.2.3 DAQ and Intermediate Controller

The intermediate controller is a National Instruments CompactRio rapid-prototyping controller. This controller provides such functionalities as real-time communication and signal processing, as well as high-speed FPGA control. These functions are utilized to collect the weight data from the CAN network of eNods, and the FPGA to control the speed of the motors through encoder feedback and analog control of

the motor drivers. CompactRio operates in a National Instruments specific IDE software, thus making it incompatible with industry equipment that typically employ industry-grade large-scale networks compatible software. This issue is discussed further in Section **Error! Reference source not found.**.

2.2.4 Vision System

A dimensioning camera, developed by an independent contractor called *Tricolops Technology*, is utilized to confirm the size and orientation of each parcel. The infrared camera calculates the length, width, height and volume of each package that passes below it, supporting up to 10 different cuboid packages at any given moment. This information is useful for Purolator to verify the size of packages, and also to determine which load cell carries each package for data singulation purposes. Purolator also requires the unique bar codes labelled on each parcel to be read, stored and associated with each package along with the corresponding weight estimate. Thus, the bar code scanners are implemented in this prototype to make it a fully functioning piece of the industrial setting of a Purolator sorting and distribution centre, though they are not relevant to this thesis.

2.3 System Integration

The completed prototype of the IMWS array is mounted to an aluminum support frame as shown in Figure 2.7. Beams of aluminum across the frame provide the mounting base for the load cells and motor drivers, while the rest of the frame support the remaining electronics. An overhead structure supports the dimensioning camera and bar code scanners. Rollers are added to the entry and exit points of the array to smoothly transition objects into and out of the system.

Figure 2.7: Final prototype of IMWS Array system

The final weight measurement array consists of 24 weight measurement cells or modules. Each module consists of a conveyor, a motor, a motor driver, a load cell, and a load cell transmitter. The conveyor/motor/load cell units are mounted in a 4x6 grid, with the motor driver mounted next to the load cell on the beam. The wiring for each unit runs along the beams to reach the transmitters and intermediate controller arranged at the front of the frame. Each load cell is wired to its own transmitter, and the transmitters are wired to a single node to form the CAN network, and this network is connected to the intermediate controller. Speed control of the motor with encoder feedback, are wired directly to the intermediate controller.

The intermediate controller requires manual activation from a laptop PC, but cannot establish a connection with the infrared camera. However, the intermediate controller is also unable to establish a direct connection with multiple PCs, and can only connect with PCs that run its specific development software. As the project is funded and operated by a corporate partner, and the integration of the camera systems belonged to another party, a host PC was required to separate that system from the university-owned equipment, and an additional license for the intermediate controller's development software could not be obtained. Therefore, the intermediate controller, with the load cell data, connects to a laptop PC via an Ethernet LAN, which is ported through a network switch. The infrared camera connects directly to the host PC, while the host PC also connects to the network switch to access the load cell data from the laptop PC through a TCP/IP network. The host PC then consolidates the load cell and camera data and provides a log file of all load cell measurements and all visible package vertices' coordinates at each sample.

Sample rate is limited by the camera's frame rate, and so while the intermediate controller can provide a load cell update every 4ms, the camera vertices data is only available every 33ms. Some load cell data is lost in the mock synchronization of the two data inputs, where the latest load cell update is logged with every camera update. Featured below in Figure 2.8 is a schematic diagram of the wiring of the system.

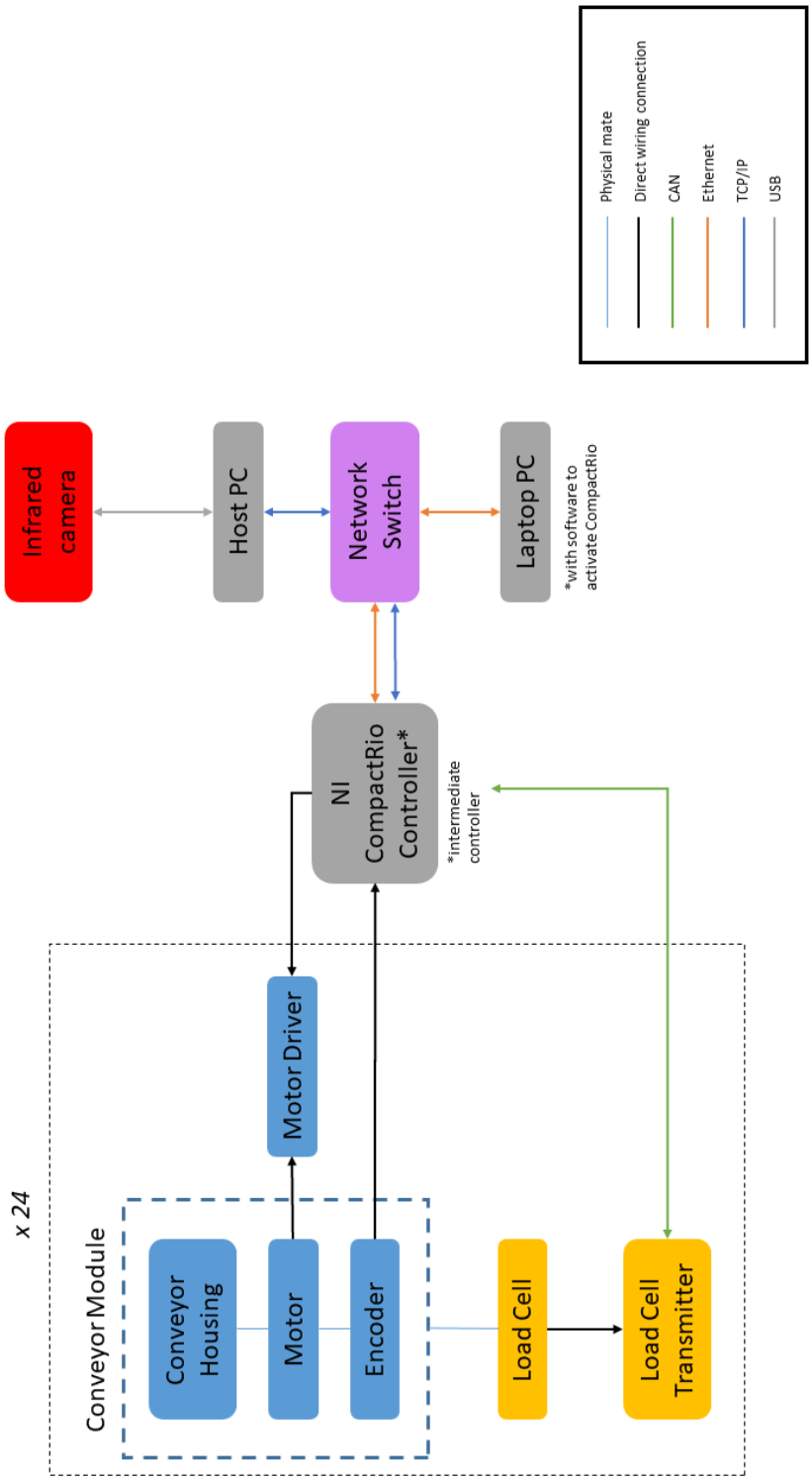

Figure 2.8: Physical and electrical connections of the IMWS array

Chapter 3
Weight Estimation

In considering how to design proper weight estimation algorithms, the work in this thesis necessitates an approach different from the typical signal processing and model-based estimation techniques which are mainly developed for singulated objects. A key technical issue in estimating the weight of an individual item using the IMWS lies in the fact that multiple boxes are supported by multiple load cells. Furthermore, the specific set of loadcells that are associated with each item (and the amount of association) continuously change as the item move on the conveyor. To address these issues, we employed the recursive least square estimation (RLSE) method. The RLSE algorithm is advantageous in determining unknown parameters when they are integrated in a set of linear equations with respect to (known) regression terms that vary with respect to time. The main idea is to associate the fraction of any object's area with the fraction of weight measurement of the corresponding load cell. This area data is combined with the load data in the least squares estimation.

Before we implement the RLSE method, we first investigated the performance of the designed IMWS array when measuring singulated packages. In the case of effective singulation, complex calculations are not required, and a simple summation of the measurements from all supporting load cells of an object will suffice. This is then used as the baseline to compare performance of the RLSE method. Investigation on the baseline performance is described in detail in Section 3.1. An overview of the RLSE method is given in Section 3.2 and the experimental results are shown in Section 3.3. Consistency in height between the individual conveyors can have a negative impact on the accuracy of weight estimation. Section 3.4 explains the effects of the leveling of conveyor height, as well as overhead camera accuracy, as challenges to the overall estimation accuracy.

In the majority of the conducted experiments, the conveyor motors are run at approximately 65rpm, resulting in a belt speed of 0.14m/s. The effects of the conveyor speed on the load measurement had already been observed and it was determined that the noise from any PWM effects or mechanical vibration (that were not attenuated by the low-pass and self-adaptive filters in the eNods) did not affect the overall median measurement, and so they can be ignored in further experiments.

Eight different packages have been assembled for the experiments, henceforth referred to as "boxes" and are used in a variety of groupings and combinations. Their information is in Table 3.1 on the following page.

Table 3.1: Weights, dimensions and other information about test boxes used in experiments

Box ID	Weight (g)	Length (mm)	Width (mm)	Height (mm)	Surface area (mm^2)	Soft or Rigid?	Mass distribution
A	1259	323	171	146	55233	rigid	uniform
B	1747	320	162	105	51840	soft	uniform
C	4029	272	208	178	56576	soft	uniform
E	2706	169	130	70	21970	rigid	non-uniform
F	722	200	137	99	27400	soft	non-uniform
G	2864	379	313	174	118627	rigid	non-uniform
U1	1311	160	160	138	25600	middle	uniform
U2	4475	301	307	111	92407	middle	uniform

3.1 Baseline Performance of IMWS Array with Singulated Boxes

To validate the system's performance in weighing multiple, non-singulated boxes, its performance as a simple checkweigher must first be determined. Moving one box across the grid will simulate the behaviour of the system as a traditional checkweigher. This type of experiment also simulates the multiple, singulated boxes case, where, in a group of boxes, only one box should be supported by any given load cell at any instance. If singulated sufficiently in the direction of travel, a preceding box will have unloaded from a conveyor and its load cell's signal returned to zero state before the subsequent box loads on. Sufficient singulation transverse to the direction of travel simply requires the boxes to travel on separate rows of conveyors. Boxes that are completed singulated from each other are exemplified in Figure 3.1.

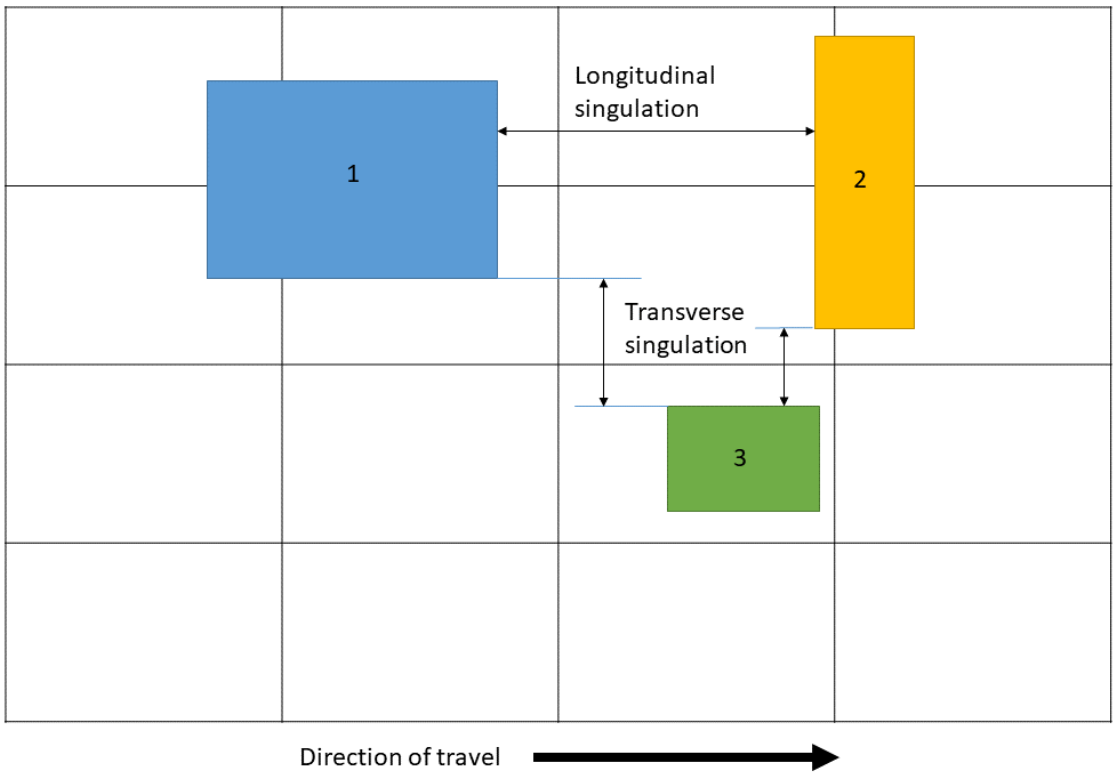

Figure 3.1: Singulation of boxes in both directions

All three boxes in Figure 3.1 above are singulated from each other in both the longitudinal direction of travel and the transverse direction. Box 1 and 3 are singulated in the transverse direction because they will never travel on the same rows of conveyors and thus do not require additional longitudinal singulation. The same goes for Box 2 and 3. Box 1 and 2 are singulated in the longitudinal direction because though they will travel on the same conveyors, they will not occupy any given load cell together at the same instance. Singulation ensures that the entirety of a load cell's measurement can be apportioned to a single box.

To estimate the weight of each singulated box, a sum must be taken of the measurements of each load cell that supports it at each instance. Then, taking the median of all of these sums will give an appropriate weight estimation. Determining the supporting load cells for a box requires the use of the overhead infrared camera. The coordinates of the four vertices of a box are compared against the four vertices of each conveyor module. If any of the box's vertices intersects with a conveyor's surface area, the corresponding load cell's data is associated with that box. In this case of singulated boxes, the entirety of

the load cell's data at that instance can be apportioned to that box. In the non-singulated case, the load cells are flagged as supporting the box, and the rest of the weight estimation combines this logic with the box's area.

In these simplest experiments, we also find a baseline for the largest impact that the levelling of the conveyor heights can have on weight measurement since the conveyor heights are not levelled precisely and the experiments involve a very rigid box. Thus the weight estimation of this rigid box exhibited an average measurement within 7.5% of the true weight, whereas the weight estimation of a softer box experienced an average measurement within 0.4%. Unlike the following experiments, these baseline tests run the conveyors at 5 graduated levels of speed within its full range of 0-0.78m/s, and so the results are truly dynamic.

Figure 3.2 on the next page shows the statistical results of the simple averaging weight estimation method for soft boxes moving at 0.14m/s only. The ends of the whiskers show the maximum and minimum error values of the statistical set; the red line indicates the median error value; and the blue rectangle delineates the 75^{th} and 25^{th} percentile values, i.e. 50% of the samples lie within this box. Despite the short heights of the blue rectangles indicating high measurement precision and the near-zero medians indicating measurement accuracy lying within 1%, the results appear to be biased to overestimate the weight of each box.

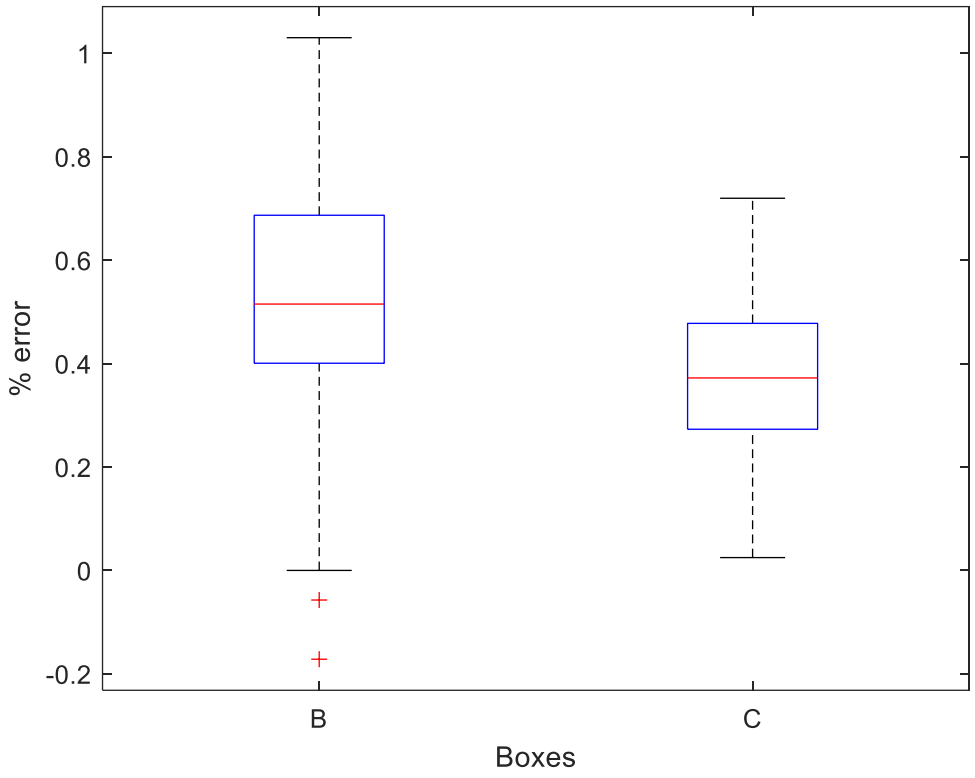

Figure 3.2: "Soft" boxes B and C exhibit estimation errors within 1% using the simple averaging method when completely singulated

3.2 Recursive Least Squares Estimation Applied to Dynamic Weighing

To implement a least squares estimation on non-singulated objects, we must assume that each object is a cuboid shape (box) with uniform density. Assume also that there are, in total, N load cells in the IMWS array system, and m boxes are moving together loaded on the system. Let us also denote by n the total number of load cells that are in contact with any package. Figure 3.3 shows an example case where $N = 16$, $m = 3$ and $n = 10$. For each box, say the j-th box ($j \in \{1, \dots, m\}$), the camera provides indices of all load cells that are supporting this box.

Let us first denote the load measurement data from the i-th load cell by L_i and the total weight of the j-th box by w_j. Note that some load cells may be supporting multiple boxes simultaneously. Let us define the fraction of the weight of the j-th box supported by the i-th load cell as α_i^j. We can simply consider that $\alpha_i^j = 0$ if the j-th box is not loaded onto the i-th load cell. Note that, by this definition α_i^j's must add

up to 1 for all i's, i.e. $\sum_i \alpha_i^j = 1$. Besides, we have the following relation between w_j and L_i:

$$L_i = \sum_{j=1}^{m} \alpha_i^j w_j\,, \qquad i = 1, \dots, N \tag{3.1}$$

Note that $\sum_i \alpha_i^j = 1$ for the j-th box. Rewriting the above equation in matrix form, we have

$$\begin{bmatrix} L_3 \\ L_4 \\ L_6 \\ L_7 \\ L_8 \\ L_{10} \\ L_{11} \\ L_{12} \\ L_{15} \\ L_{16} \end{bmatrix} = \begin{bmatrix} 0 & \alpha_3^2 & 0 \\ 0 & \alpha_4^2 & 0 \\ 0 & 0 & \alpha_6^3 \\ 0 & \alpha_7^2 & \alpha_7^3 \\ 0 & \alpha_8^2 & 0 \\ 0 & 0 & \alpha_{10}^3 \\ \alpha_{11}^1 & 0 & \alpha_{11}^3 \\ \alpha_{12}^1 & 0 & 0 \\ \alpha_{15}^1 & 0 & 0 \\ \alpha_{16}^1 & 0 & 0 \end{bmatrix} \begin{bmatrix} w_1 \\ w_2 \\ w_3 \end{bmatrix}, \quad \text{with } \sum_i \alpha_i^j = 1 \tag{3.2}$$

which can be rewritten in a more compact form as $\Lambda = A\mathrm{W}$ $(\Lambda \in \mathbb{R}^n,\ A \in \mathbb{R}^{n\times m}, \mathrm{W} \in \mathbb{R}^m)$. Note that the matrix A is always 'skinny' (i.e. the number of rows is always greater than or equal to that of columns, or $n \geq m$) because each box must be supported by at least one load cell. In fact, when we have $n = m$, we have a situation where all boxes are singulated. Also, if the size of the box is larger than a half of the size of the load cell, then we can assure that each column of the matrix A is always independent from others. Therefore, we can always have a solution for the weight vector $W = [w_1, \dots, w_m]^T$ by the least-square,

$$\widehat{W} = \min_W \|\Lambda - AW\|^2 \tag{3.3}$$

the solution of which is given by the pseudo-inverse of A as

$$\widehat{W} = (A^T A)^{-1} A^T \Lambda \tag{3.4}$$

where the hat notation stands for the estimation of the corresponding values. Note that we can obtain this solution for every sample time of the weight data.

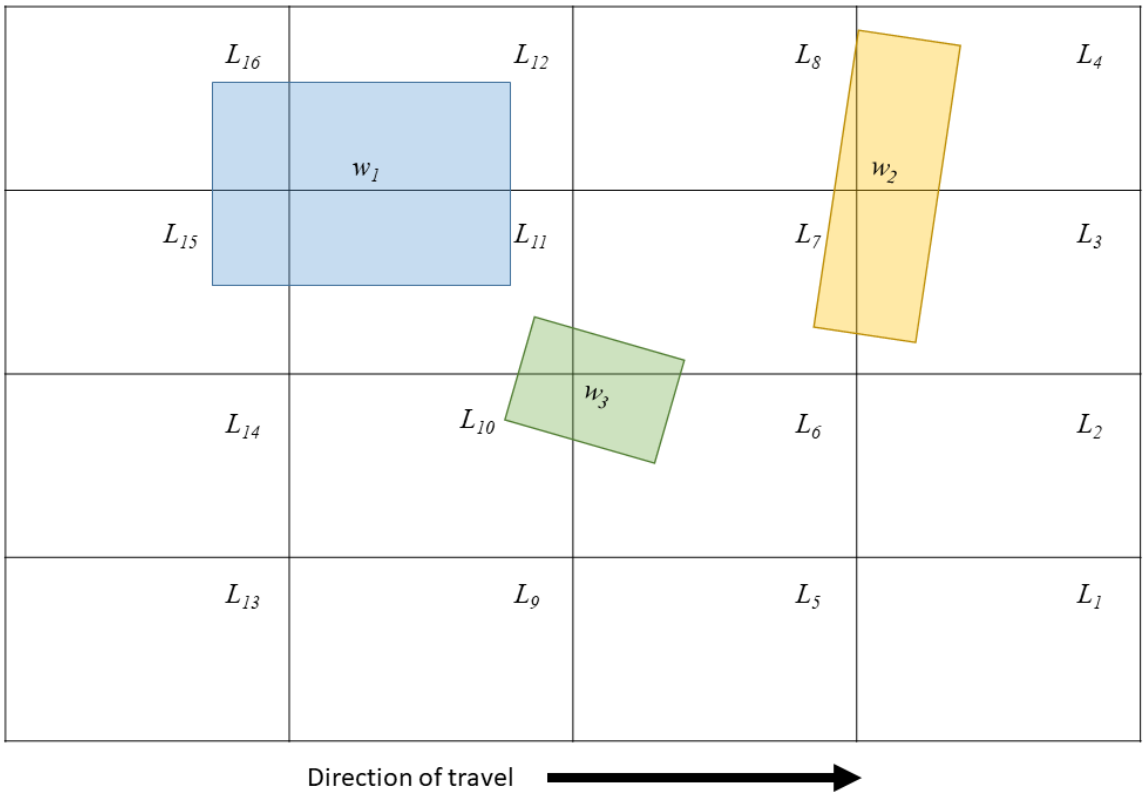

Figure 3.3: Example non-singulated case

Since the weight measurement vector Λ and the fraction matrix A are coming in as a stream of data, we have a large number of measurement from which we can further refine our weight estimation. Therefore, we can run this least-square solution in a recursive way making it as a RLS algorithm. In the RLS approach, we also need to consider the discontinuity in the size of Λ and A as the number 'n' is a discontinuous (or more specifically, piecewise-constant) function of time.

Now, let us denote by k the discrete-time index, i.e. $t = kT_s$ where T_s is the sample time. Since the regression matrix A and the load cell vector Λ (as well as 'n', the number of rows of A) vary with time, we can let them as functions of time, $\Lambda \to \Lambda(k), A \to A(k)$ and $n \to n(k)$. Then, the RLS problem can be stated as [31]:

$$\widehat{W}(N_f) = \min_{W} \sum_{k=1}^{N_f} \|\Lambda(\mathrm{k}) - A(k)W\|^2 \tag{3.5}$$

where N_f denotes the final time index. The solution to (5.3) can be given in a recursive way as

$$\widehat{W}(k) = \widehat{W}(k-1) + K(k)\left(\Lambda(k) - A(k)\widehat{W}(k-1)\right), \tag{3.6a}$$

$$K(k) = P(k)A(k)^T = P(k-1)A(k)^T\left(I_{n(k)} + A(k)P(k-1)A(k)^T\right)^{-1}, \tag{3.6b}$$

$$\begin{aligned} P(k) &= P(k-1) - P(k-1)A(k)^T\left(I_{n(k)} + A(k)P(k-1)A(k)^T\right)^{-1}A(k)P(k-1) \\ &= \left(I_{n(k)} - K(k)A(k)^T\right)P(k-1) \end{aligned} \tag{3.6d}$$

where $I_{n(k)}$ is the identity matrix with its size $n(k) \times n(k)$ and the initial value for the recursion matrix $P(k) \in \mathbb{R}^{m\times m}$, i.e. $P(0)$ needs to be selected as a positive definite matrix.

3.3 Experimental Validation of Recursive Least Squares Estimation Algorithm

A series of different experiment sets were conducted to capture the overall and specific performance of the IMWS array. These experiments involved a large variety of groupings and combinations, orientations, and positions of the test boxes as they travel through the system, generating a large number of data sets to observe. Post-processing of each data set to produce the weight estimates of the participating boxes is achieved with MATLAB, a multi-paradigm numerical computing environment by MathWorks Inc. The MATLAB script is specifically programmed to extract, associate, and manipulate the data and pass it through a coded array-based implementation of the RLSE algorithm. The script also produces the convergence plots for the weight estimates of each participating box in the given experiment, and saves the results to be analyzed further in a separate script with a statistical perspective.

First, we observe the performance of the RLSE algorithm with singulated boxes in Figure 3.4 on the following page, as compared to the baseline performance in Figure 3.2.

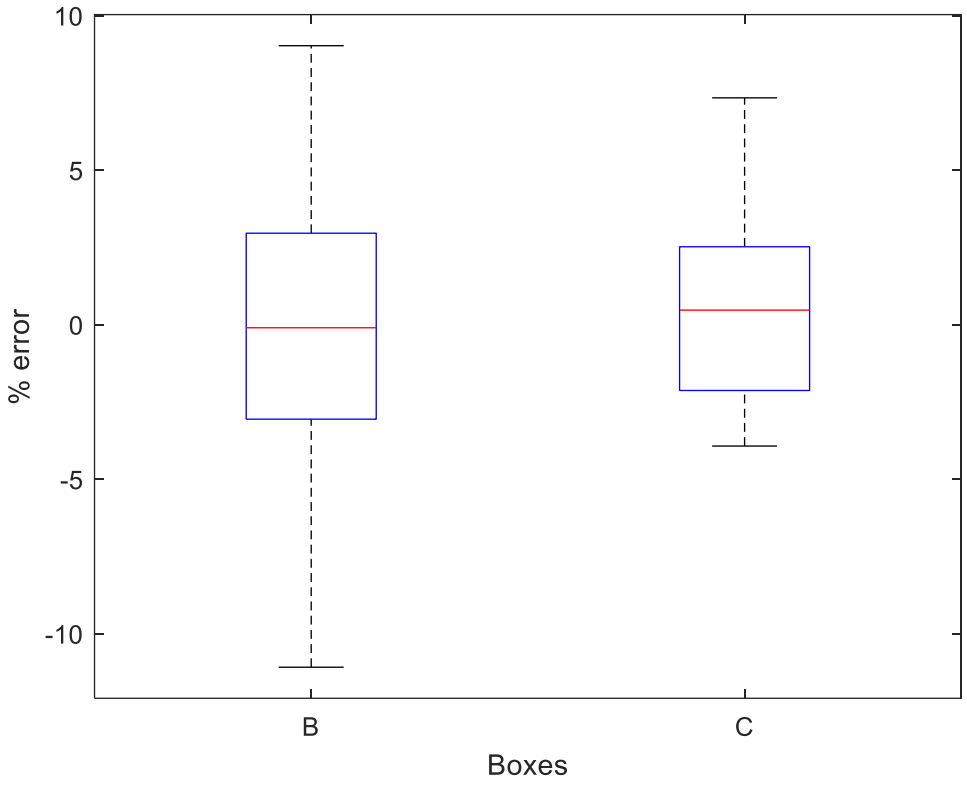

Figure 3.4: Estimation error of singulated boxes, using RLS estimation method

Figure 3.4 shows that although the range of error is larger than the baseline performance (thus both precision and accuracy have suffered), the RLSE method produces close to zero-median error for the singulated cases.

When testing multiple boxes at a time, a minimum spacing of 25mm was maintained so that each box could be detected individually by the infrared camera that provides the box locations, and consequently their portions of area supported by specific load cells could be determined. The multiple, non-singulated cases involve either three or four boxes travelling through the IMWS array, where their full areas are observed within the camera space for a determinable duration of time (i.e. in this duration of interest, all of the boxes are completely supported by the array and are not transitioning in or out of the array). Examples of these differing cases are shown below in Figure 3.5-Figure 3.8 and their corresponding weight estimation results of the RLSE algorithm are shown in Figure 3.9 and Figure 3.10. The images from the overhead camera feed are flipped vertically. The algorithm will only estimate the weight during

the period that all boxes are completely supported by the grid and in view of the camera. We opt not use Box A in these experiments because it is indeed not only just a rigid box, but a completely uniform rigid body and will continue to provide unfavourable results. Despite the conveyor heights having now been levelled to the best of human ability, the unforgiving rigidity of Box A would skew results.

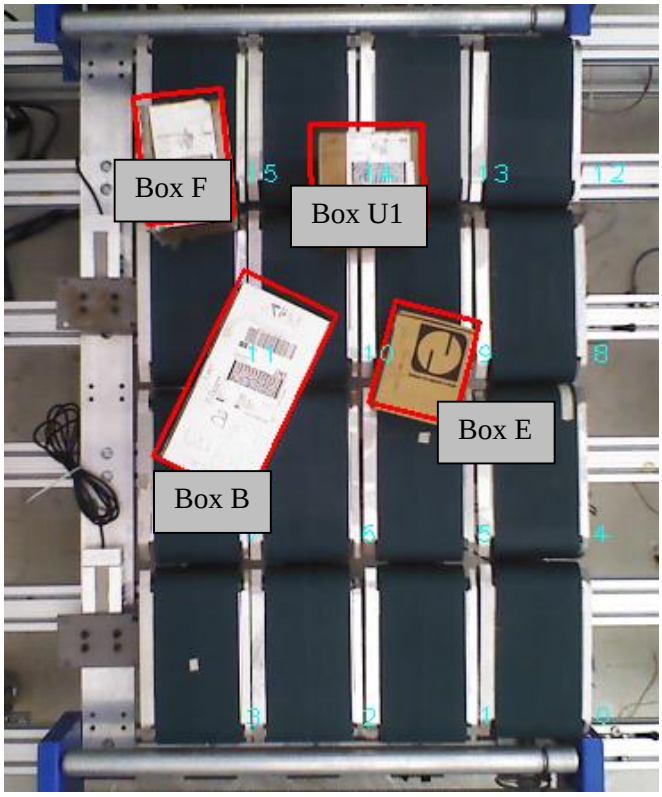

Figure 3.5: Overhead image of an experiment involving four boxes: B, E, F, and U1

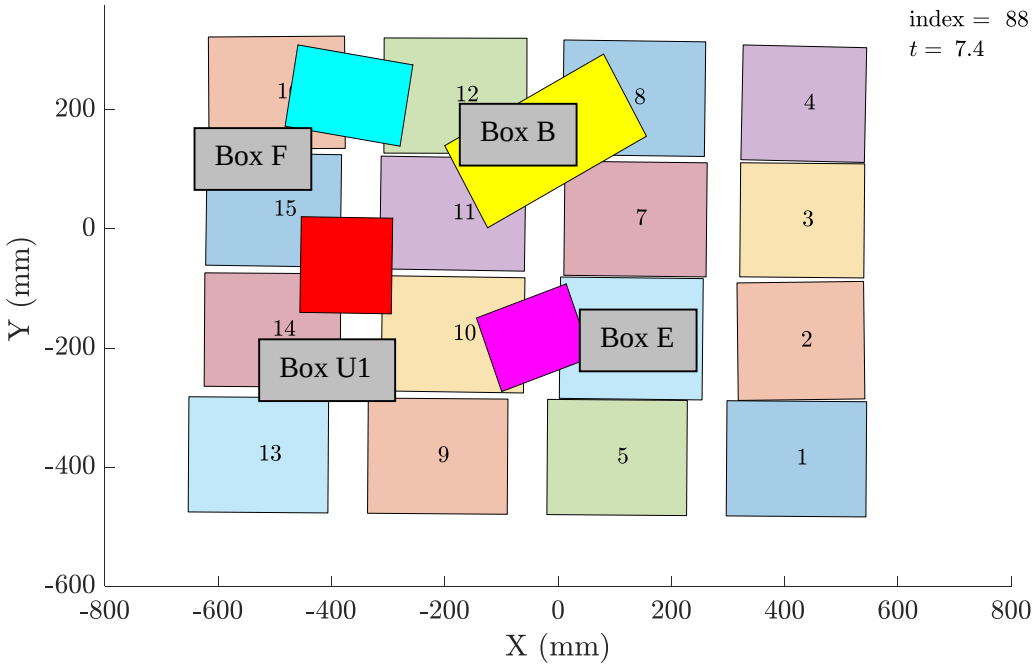

Figure 3.6: Rendering of box positions in previous figure with respect to true conveyor positions

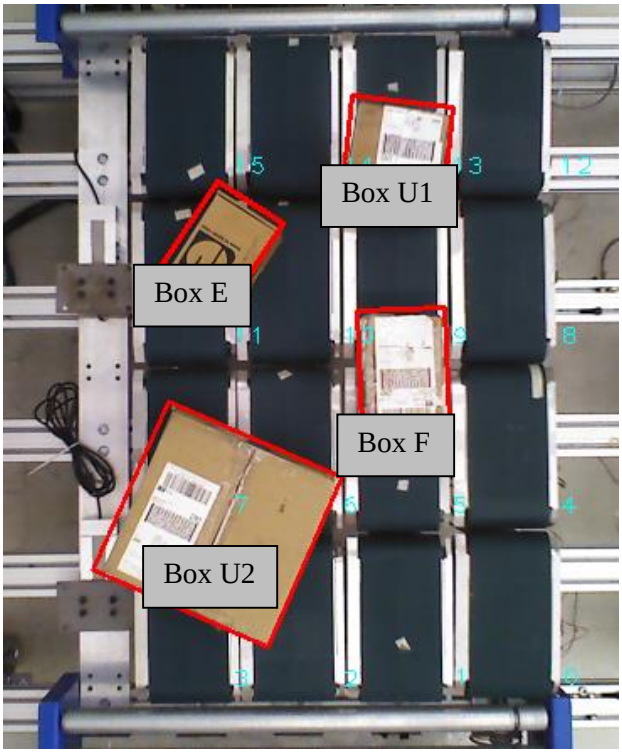

Figure 3.7: Overhead image of an experiment involving four boxes: E, F, U1 and U2.

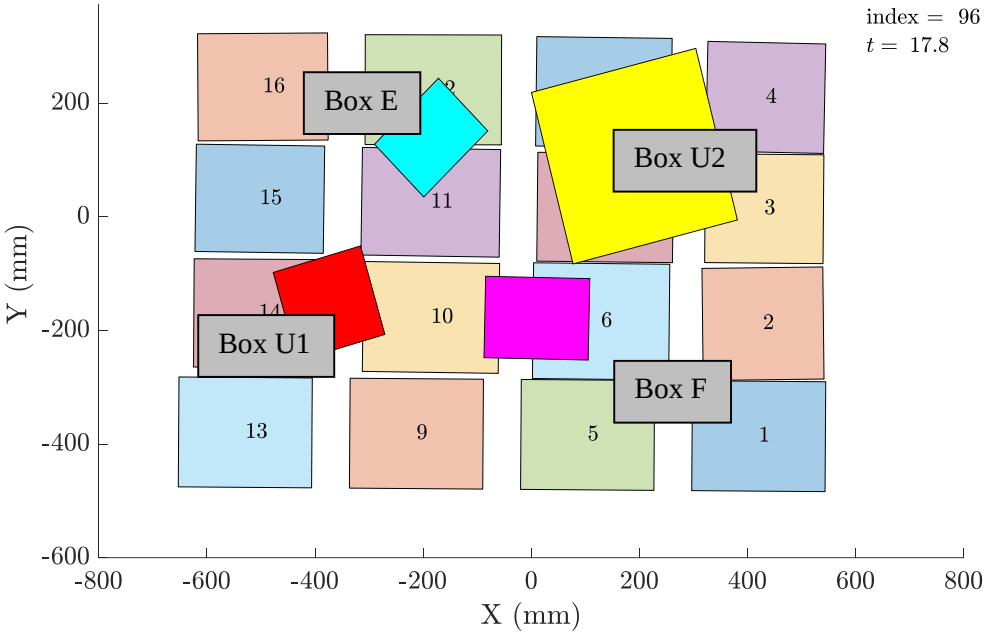

Figure 3.8: Rendering of box positions in previous figure with respect to true conveyor positions

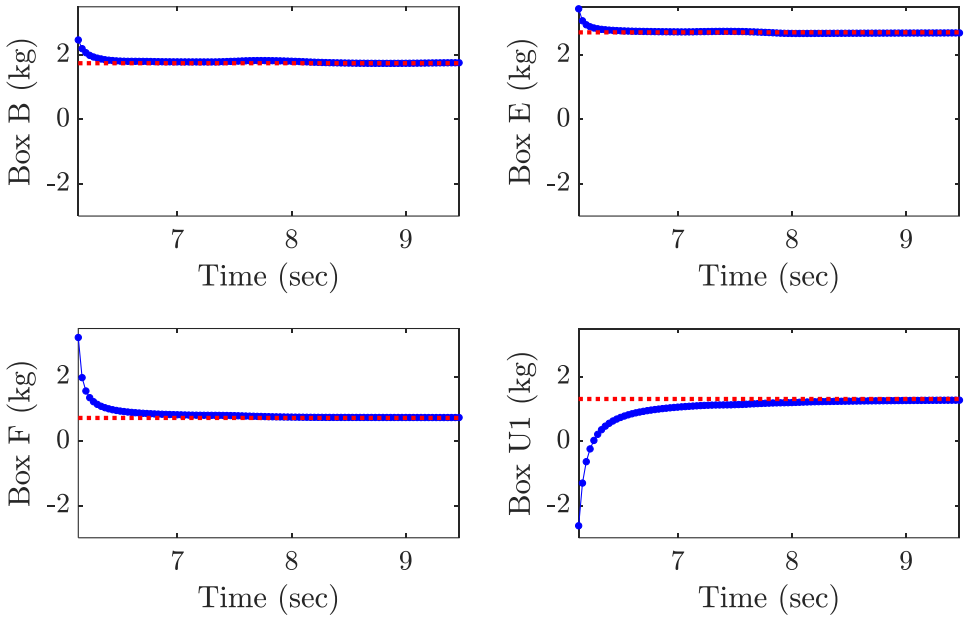

Figure 3.9: Result of RLS weight estimation for experiment containing boxes B, E, F, and U1. Red is the true weight and blue is the RLSE result.

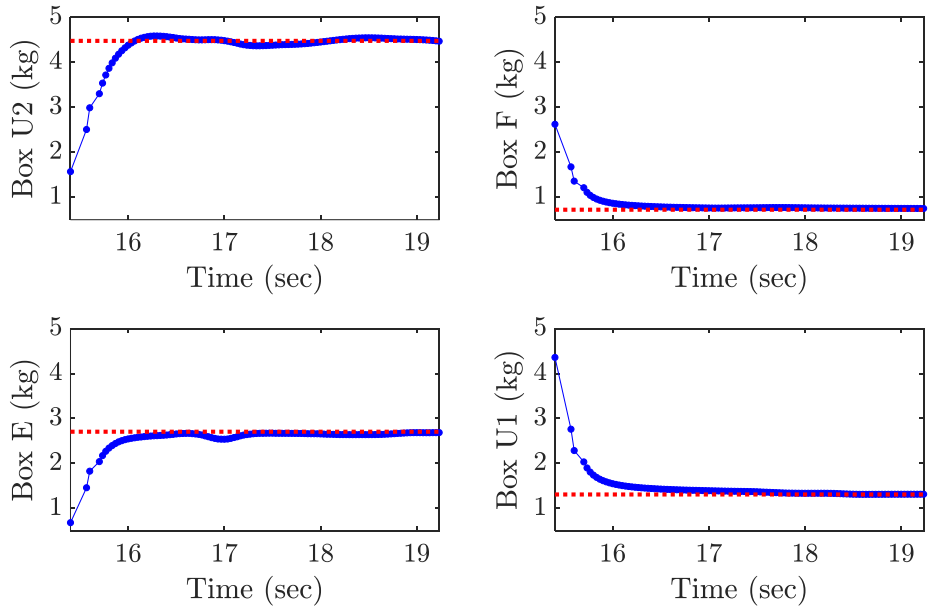

Figure 3.10: Result of RLS weight estimation for experiment containing boxes E, F, U1 and U2. Red is the true weight and blue is the RLSE result.

As demonstrated by Figure 3.9 and Figure 3.10, the algorithm improves upon the previous weight estimates and the estimate becomes more accurate with time, with the final estimation value as the most accurate weight estimate. The initial value of the recursion matrix $P(k) \in \mathbb{R}^{m \times m}$ affects the speed of convergence of the estimate signal, while the initial value of the recursive estimate $\widehat{W}(k)$ to be used in the first sample has a significant impact on the range within which the estimate signal is found, and thus impacts the final weight estimate. If we assume that absolutely no information is known about the boxes that enter the IMWS array, then there is no deterministic method of finding an initial value for $\widehat{W}(k)$, so its initial value must be randomized. Figure 3.9 and Figure 3.10 are examples of randomized initial values of $\widehat{W}(k)$.

If we can assume that the IMWS array will be used in an environment where the some general estimate of the boxes' weight is available and associated with the appropriate boxes, then that general estimate can be used as the initial value of $\widehat{W}(k)$. In fact, the eventual industrial application of the IMWS array demands that bar code stickers will have already been applied to the boxes and a bar code scanner will identify the boxes. These bar codes contain the information declared by the customer (dimensions and weight) which can be assumed to be very rough estimates within 30% of the true measurements. Assuming that this information is available to the computing system that implements the RLS estimation algorithm, we can then use the customer-declared weight for each box as the initial value of $\widehat{W}(k)$. We can compare the effectiveness of using a rough estimate as the initial estimation value versus using a random value, by observing the consolidation of estimation errors shown in the figures on the following pages.

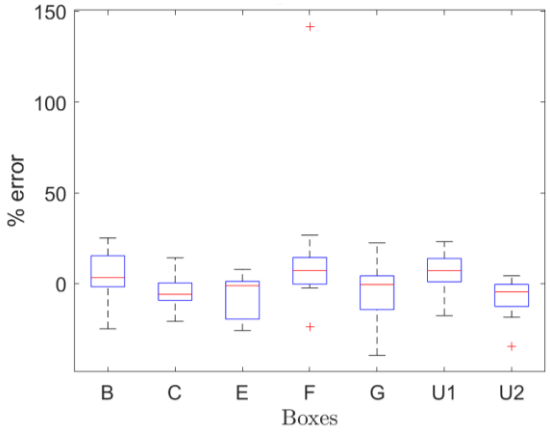

Figure 3.11: Statistical analysis of final estimation of each box as they travel in groups of 3, using randomized initial estimate

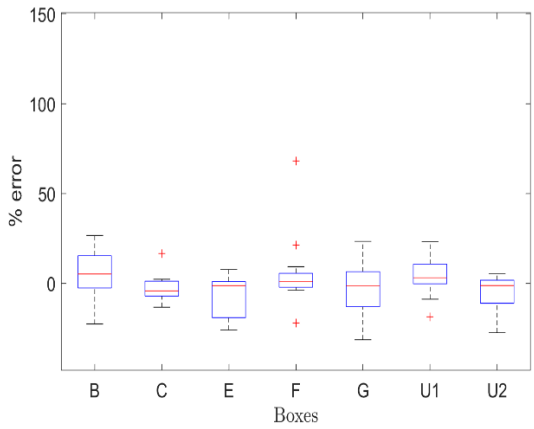

Figure 3.12: Statistical analysis of final estimation of each box as they travel in groups of 3, using initial estimate roughly close to true weight

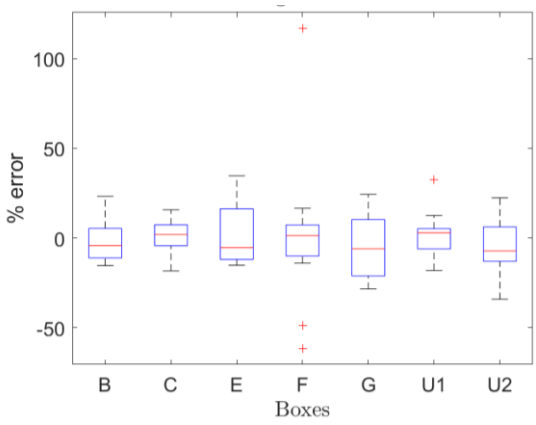

Figure 3.13: Statistical analysis of final estimation of each box as they travel in groups of 4, using randomized initial estimate

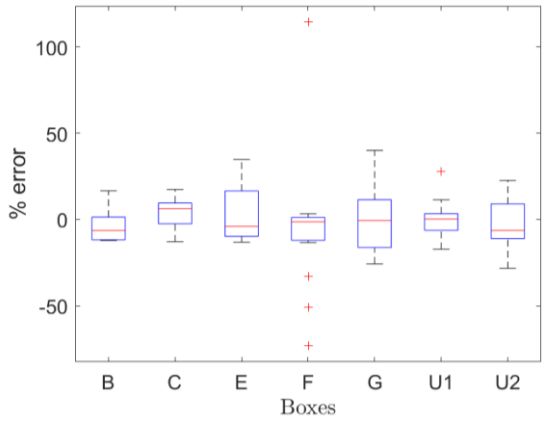

Figure 3.14: Statistical analysis of final estimation of each box as they travel in groups of 4, using initial estimate roughly close to true weight

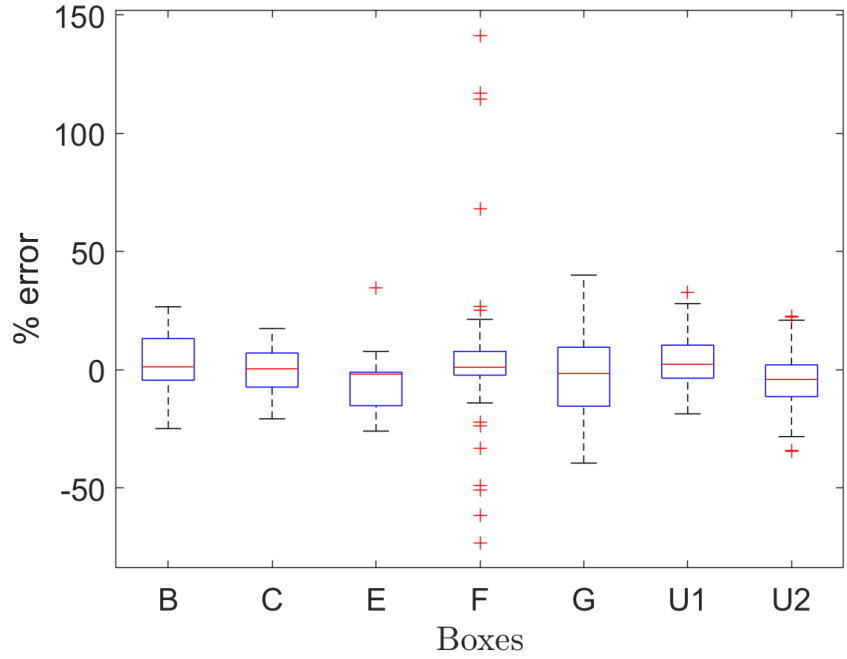

Figure 3.15: Statistical analysis of final estimation of each box across all experiments. Each box appears in a minimum of 50 experiments

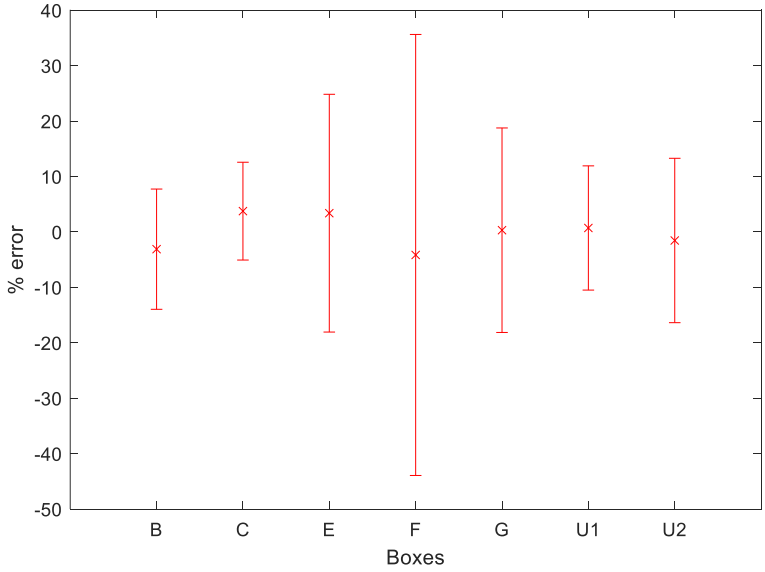

Figure 3.16: Alternate visualization of the data in Figure 3.15. Whiskers show the standard deviation of each statistical set, and the X's indicate mean

The results in Figure 3.11 - Figure 3.14 show that the RLS estimation maintains near-zero mean error and that using a close weight estimate as the initial value does increase the precision of the estimates, demonstrated by the decreased size of the blue rectangles (i.e. a closer grouping of the estimate errors), though it does not provide significant improvement in the estimation accuracy, as seen in the unchanging medians.

When we consolidate the data from all of the experiments and analyses, as shown in Figure 3.15 and Figure 3.16, we can make observations on the effects of the properties of the test boxes. Box F experiences the most outliers because of its small size: it is difficult for the camera to accurately detect its position and even slight deviations cause larger errors in the determination of area fractions. It is also the lightest box in the test group, and is more susceptible to noise. There may be outliers in the analysis of Box U1 and Box E because of the boxes' rigidity. Box F and U1 are usually overestimated, due to their small size: more load is incorrectly attributed to them when their locations (as thus their supported areas) are inaccurately measured by the camera.

Thus, we can say that in these experimental sets, the boxes that are most likely to have their weights estimated correctly are those that are not small (Box B with a surface area of 51840mm^2 exemplifies the boundary of this lower limit) and not light (Box F with 722g is below this limit, but U1 with 1311g would be acceptable). This corresponds to specifications of a surface area that spans at least 0.05m^2 and a weight of at least 1kg.

Box G experiences the lowest precision because its weight is not uniformly distributed within its large area, and so the product it carries is able to shift while traveling. The number of boxes in each experiment (three versus four) does not seem to have a significant impact on the overall accuracy, though it does come into play when considering the available spacing between boxes. That is, experiments where boxes are arranged closer together may exhibit lower estimation accuracy.

3.4 Structural Factors that Affect Estimation Accuracy

The fundamental array structure of the IMWS array introduces two mechanical issues that are not present in the traditional single checkweigher problem. The first challenge is the levelling of the individual conveyor modules; that is, maintaining a consistent height of all flat, top surfaces of conveyors when assembling the system. Since these modules are assembled by hand, it is difficult to adjust them precisely enough to achieve the exact same height on each. The mounting L-brackets are slotted to allow for height

adjustment, based on calibration requirements and depth sensitivity of the camera, and so a common fixed position is difficult to achieve and maintain across multiple conveyor modules.

The next challenge compounds on the first, when a package is so rigid that it will not yield to the differences in the terrain it travels, and thus can become supported by only the conveyors with the tallest height even when its surface area appears to overlap with multiple conveyors. The less rigid a package is, the better its soft edges can conform to the step created between two conveyors of differing height and its weight can be supported by both conveyors. A rigid package would be lifted up by the tallest conveyor, where the majority of its load would rest, leaving very little load (while the package transitions up to half of its load onto the taller conveyor, or while the centre of mass (COM) is still positioned over the shorter conveyor) to no load (when half or more of the package is supported by the taller conveyor, or when the COM is positioned over the taller conveyor) for the shorter conveyor. To understand the leveling issue in a more detail, Figure 3.17 illustrates the effects of inconsistent heights between conveyors.

Side	Overhead
	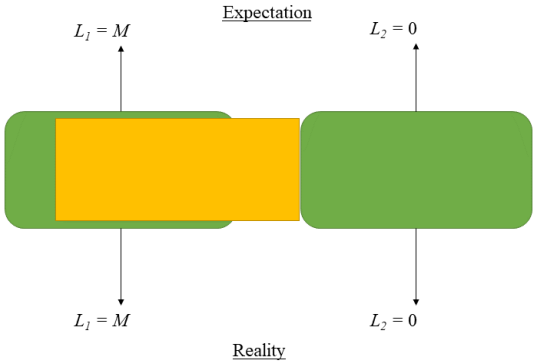
a) Package (yellow) is fully supported by the first conveyor. Expectation matches reality.	
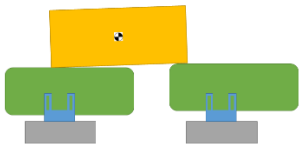	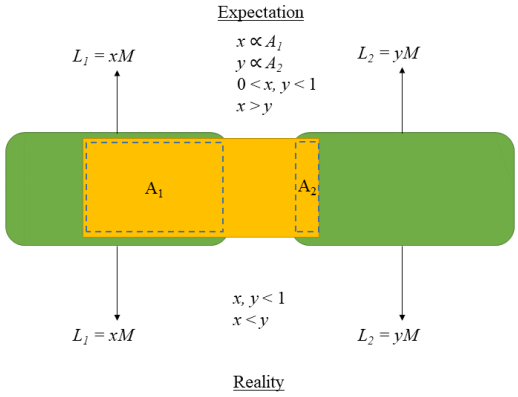
b) Package transitions from shorter, first conveyor to taller, second conveyor. Reality no longer follows expectation, based on supported area of package.	
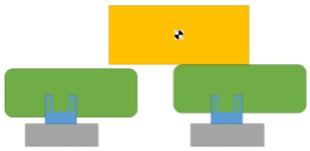	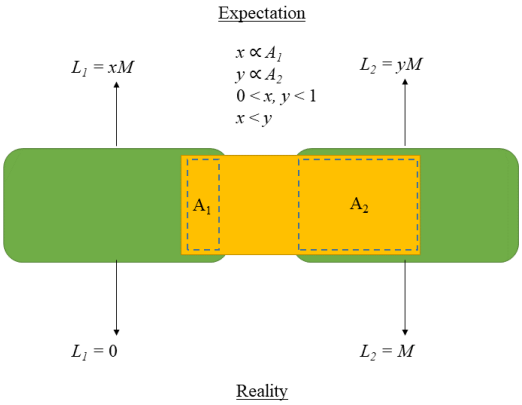
c) Package appears to be supported by both conveyors, but has transitioned fully to the taller, second conveyor.	

Figure 3.17: Difference in weight estimation due to leveling error

When the package is fully supported by the first conveyor, which is shorter in height than the second conveyor, the weight measurement from the first load cell, L_1, is equal to the total weight of the package, M, and L_2 is zero. When the package is transitioning from the shorter conveyor to the taller conveyor, the load distribution shifts from conveyor 1 to conveyor 2. This is not an even distribution and is heavily dependent on the package's COM. If using the overlapping areas of the package with the respective conveyors, then it would seem that conveyor 1 would support more of the load than conveyor 2, but this may not be the case, considering the mass distribution of the package. In any case, the load on a conveyor is no longer proportional to the supported area of the package. In part c) of Figure 3.16, the package has fully transitioned to conveyor 2, though from the overhead view it would seem it is still supported by conveyor 1 as well.

These challenges can be avoided in a further iteration of the prototype, where the height of each individual conveyor is fixed in manufacturing instead of adjustable by the user. If adjustability is still required, then some graduated marked scale on the L-brackets would allow one to initially assemble each conveyor using the same height reference, rather than retroactively adjusting the heights of conveyors to match each other. The combined challenges of the conveyor level and rigidity of the packages to be measured are explored in the experiments that follow. A great effort has been made to level the conveyors at the same height, however human error that causes discrepancies of even millimetres alters the overall flatness of the system's surface and causes a multitude of weight estimation errors.

Another challenge to the accuracy of the IMWS array is the inherent accuracy of the infrared camera. The camera is used to find the locations and surface areas of the packages and conveyor modules and so a high level of accuracy is critical to ensure that the correct load measurements are apportioned to the appropriate packages. The camera boasts a resolution of ±5mm, however this seems to change when the detected object is not directly below the camera; that is, the camera's highest measurement accuracy is achieved when detected objects are around the centre of its view, closest to the infrared laser, as compared to the edges of the camera vision.

To observe these effects, we pay close attention to the position of each detected package as it moves through the system: is it in the entry section of camera space, the centre, or the exit. Figure 3.18 - Figure 3.20 show, for singulated boxes, the difference in estimation error between measurements taken from the entry section of the IMWS array, versus the center section directly below the camera, versus the exit section of the IMWS array. The measurements taken from the center of the array produce results that are zero-median, and so show promise for greater accuracy, whereas the measurements from the entry section

tend to overestimate the weights of the boxes and the exit section tends to underestimate the weights. Though it has been observed to exhibit low precision across a collection of samples, the camera's measurement precision does not seem to differ significantly between the three sections, and so there can be no comment made on the precision of the RLSE algorithm based on boxes' lateral distances from the camera's focal center.

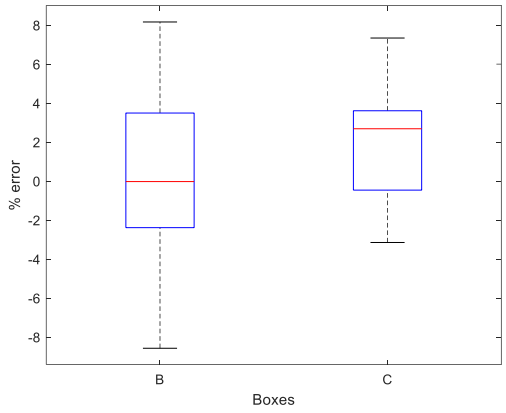

Figure 3.18: Estimation error from entry section of IMWS array

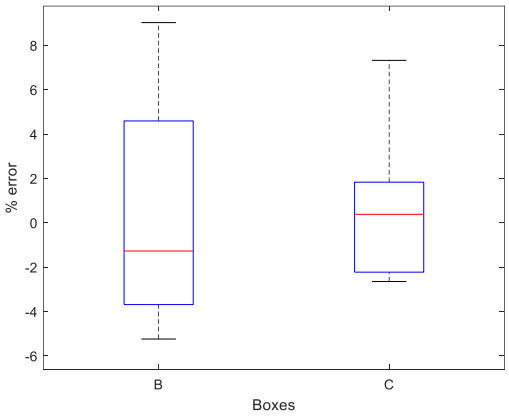

Figure 3.19: : Estimation error from center section of IMWS array

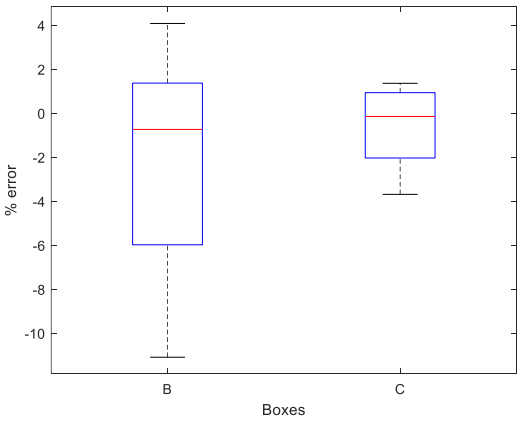

Figure 3.20: : Estimation error from exit section of IMWS array

Furthermore, it was crucial to find the true camera space coordinates of the flattest surface of the conveyor. Initially, the infrared camera system assumes that the conveyor and load cell modules are arranged in a perfect grid, and does not consider the physical gaps present between conveyors that are required to accommodate the moving parts when assembling the system. This is an inaccurate locating method, because it skews the fractional loading estimate that is associated with the area of the package supported by a conveyor. With further tuning, the camera then pinpoints the realistic positions of the conveyors within the gaps and estimates the footprint of the conveyor to include the space occupied by the driving and driven roller. However, the true load supporting area of the conveyor is only contained within the flat surface of its top, not including the driving and driven rollers. The difference between the assumed, tuned, and true load supporting conveyor positions are shown in Figure 3.21.

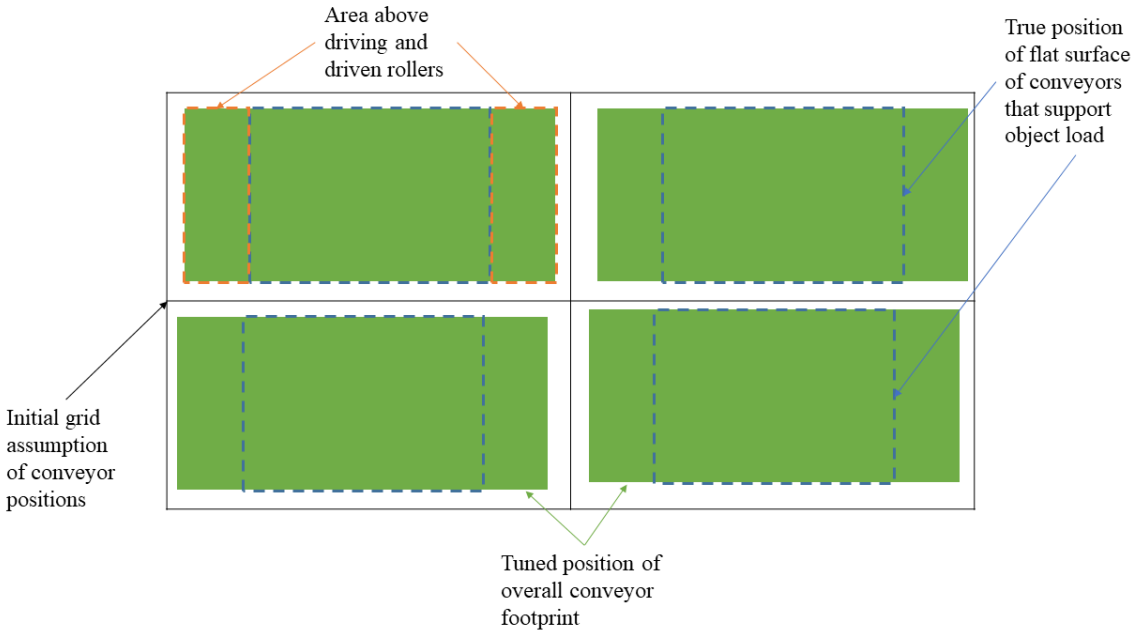

Figure 3.21: Simplified and exaggerated comparison of the initially assumed, tuned, and true positions of the supporting area of conveyors

Figure 3.21 also exhibits the effects of human error: the conveyor footprints are not centered in the grid cells, as expected, but are offset slightly because of discrepancies during assembly. These discrepancies are no longer significant when the footprint locations are known, but they would cause errors if the area estimation of the packages assumed centralized load support, apportioning more of the package load to one cell than it actually carries. When a package is supported by the flat surface of the conveyor but

overlaps with the air above the driving or driven roller, all of its supported area (and thus load) should be attributed to the flat surface only. The crucial point to note here is that the area above the rollers support no load.

In Figure 3.22, it appears as though the package is positioned directly in between the two conveyors, so that each conveyor supports approximately half of the load. Assuming that the entire footprint of the conveyor supports the package leads to attributing 45% of the package's area to each conveyor, leaving 10% unsupported. This would mean that the entire load of the package is distributed over 90% of its area. However, the true package area supported by each conveyor is in fact only 30% each. In this case where the package is positioned equally on each conveyor, this difference in area fractions is not significant to the weight estimation.

On the other hand, in the case shown in Figure 3.23, the load and area distribution across the two conveyors is clearly no longer equal, where area fractions favour the conveyor on the right, but using the footprint method skews the ratio of load on the right:left so that the load is less concentrated on the right (1.25:1), when it is in fact more concentrated (1.4:1). It is also clear to see that using the footprint method can attribute package load to a conveyor that may not support the package at all. Knowing the true locations of these flat surfaces prevents errors due to the incorrectly apportioning load fractions proportional to the assumed supported area fraction.

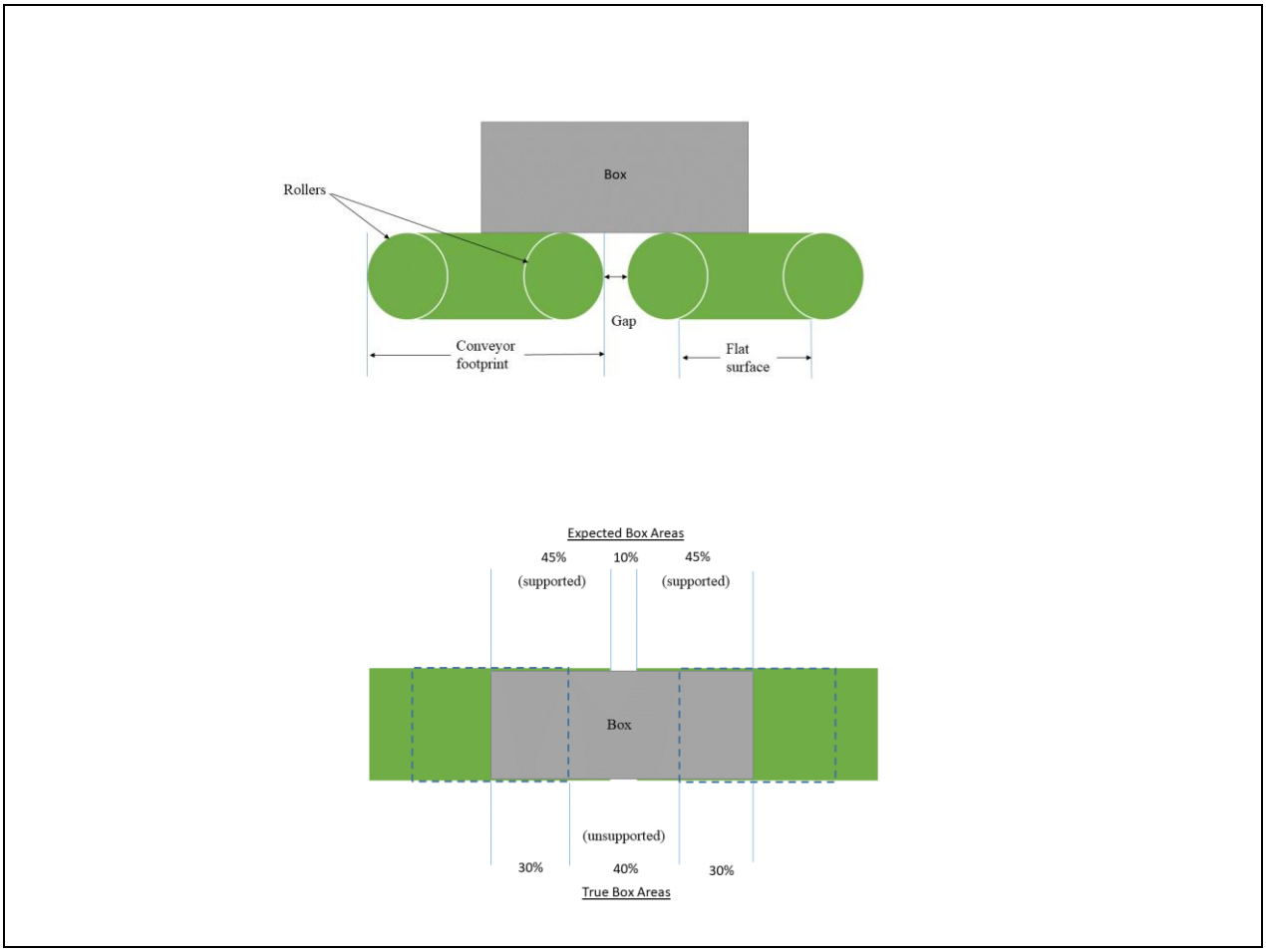

Figure 3.22: Effect of using flat surface versus entire footprint as supporting area for equally distributed package (box) case

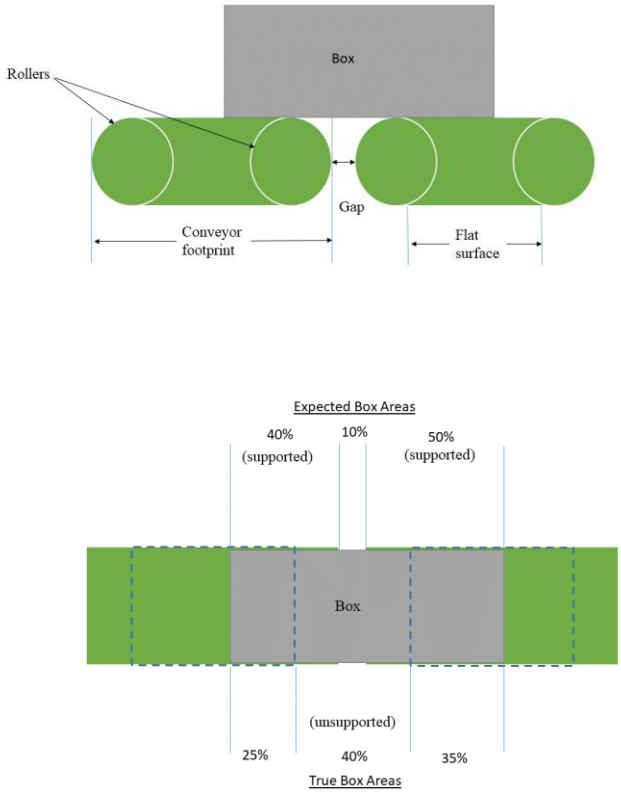

Figure 3.23: Effect of using flat surface versus entire footprint as supporting area for unequally distributed package (box) case

Chapter 4
Conclusions and Recommendations

As expected, the properties of the objects that are measured in the IMWS array can affect the efficacy of the weight estimation processed by the recursive least squares estimation (RLSE) algorithm. The algorithm is most effective for non-rigid, mid-size boxes with a generally uniform weight distribution. Higher rigidity, smaller size, and non-uniform weight distribution of the box all compromise the accuracy and precision of the estimation. Large but non-uniform boxes seem to break this rule, as the product inside the boxes have more room to shift if not properly secured, diminishing the precision of its weight estimation. Smaller boxes tend to keep the product steady within their compact form. As a method for estimating the weight of multiple objects as they pass through a system in a non-singulated manner, the RLS estimation algorithm that combines load data and supported area fractions is generally effective, typically producing measurement errors within 10%. The ideal package whose weight can be estimated with the highest accuracy and precision is one whose surface area is at least $0.05m^2$ and whose true weight lies within the range of 1-3kg.

Despite the conditions of an ideal package, the most impactful deterrents to weight estimation accuracy are inconsistent conveyor heights. Any discrepancy in height, thus creating an uneven array, causes the load distribution of packages to shift dramatically to those conveyors with the tallest surfaces. This unprecedented load distribution decreases the accuracy of the recursive lease squares algorithm, which assumes that the package areas that overlap with load areas are equivalent to the supported area of a package and is representative of a proportional fraction of the load. An uneven transition from one conveyor to the other can completely remove the load from the lower conveyor as a package leaves it, completely skewing the estimation in that instance.

The uneven leveling of the conveyors can also introduce large fluctuations in individual load cell signals when a package bumps into the edge of a conveyor taller than the one it is leaving, and when it falls onto a conveyor lower than the one it is leaving. Thus, further modelling is required of the shifting load dynamics and impact that is caused by the tilting effect due to the uneven conveyor heights. The models prescribed in [26] are a start, but even they assume that the infeed and outfeed conveyors are of a same height with the weighing conveyor. Therefore, it is imperative that the designs of the conveyor module and IMWS array system as a whole are refined to ensure that all cells of the array are identical in height, with no room for human error in the assembly of the system. It is recommended to lean towards a design

for easy assembly that either provides a reference point in order to achieve the same height in an adjustable system, or removes the adjustability altogether and leaves the conveyor height fixed. However, the original need for height adjustability was a product of the resolution and accuracy of the overhead infrared dimensioning camera, which poses some issues of its own, seen in the following paragraph.

The next most crucial factor in the accuracy of the recursive lease square estimation algorithm is the accuracy of the locations of the packages and supporting conveyors. Inaccurate locations can contribute to incorrectly attributing package loads to empty load cells and incorrectly attributing area fractions, and thus incorrectly estimating the package weight. The camera precision also suffers, as it tends to experience a significant amount of measurement noise, enough to yield package sizes that are noticeably inconsistent across a single experiment. Therefore, the package locations provided by the camera cannot be trusted to be exactly true. The first step to more accurate and precise area data would involve reducing this camera noise.

Furthermore, it seems that the camera's accuracy is best when detecting objects that are directly below it and within its focal center. It is expected that the further the object surface is from the camera lens, the less accurate its measurement and corner detection, thus why shorter packages tend to have poor detection when compared to taller packages. In addition to this longitudinal relation, it would also seem that the more removed from the center of the camera line of vision, the higher the estimation errors. This can be confirmed with further experiments to confirm the exact relationship between detection accuracy and object lateral distance from the center of the camera.

The ability to accurately estimate weight of objects with non-uniform weight distribution would truly bring the IMWS array system to peak performance. Initially, the system behaviour with non-uniform objects must be modelled by running experiments with boxes that are divided internally into discrete sections of differing masses so that the distribution is known. If successful, the duration of the estimation will not only estimate the total weight of the package, but to also determine a function for the general distribution of its weight.

The non-uniformly distributed object estimation can be attempted with the RLSE algorithm outlined in this thesis, modified without the assumption of uniform weight distribution, but it would also be interesting to implement a separate (or combined) adaptive neuro-fuzzy inference system (ANFIS). The robustness of such a system as a signal filter for the various dynamics of singulated packages travelling over a checkweigher is shown in [28], however there is no implementation designed to estimate non-singulated groups of packages. A quick study was performed using the IMWS array, in addition to this thesis' work,

investigating the training of neural networks to estimate the weight of several different groupings and combinations of boxes. It was found that this specific method of supervised learning is only effective in estimating the weights of boxes that are members of the training set. That is, the system only accurately estimates the weights of packages that it was trained with and is familiar with. Therefore, an ANFIS implementation with a heavy lean on the fuzzy-inference can introduce online learning and weight estimation of boxes outside of the training set, and drastically improve the weight estimation of foreign objects.

References

[1] Weighing & Force Measurement Panel, "A Guide to Dynamic Weighing for Industry," The Institute of Measurement and Control, London, 2010.

[2] R. Schwartz, "Automatic weighing principles, applications & developments," in *Procedings of XVI IMEKO World Congress*, Vienna, 2000.

[3] C. J. Laird, A. S. Vicencio and K. E. Serjeanston, "System, method, and computer readable medium for determining the weight of items in a non-singulated and non-spaced arrangement on a conveyor system". Canada Patent US 9,146,146 B2, 29 September 2015.

[4] IndiaMart, "Online Check Weigher," , . [Online]. Available: https://www.indiamart.com/proddetail/online-check-weigher-15762544373.html. [Accessed 06 07 2018].

[5] Griffith Elder and Company Ltd, "New Weighbridge from Griffith Elder Takes Portability to the Next Level," , 07 10 2013. [Online]. Available: https://www.weighingreview.com/article/new-weighbridge-from-griffith-elder-takes-portability-to-the-next-level. [Accessed 06 07 2018].

[6] Mettler Toledo, "CSN210 MassFlow - Overview," [Online]. Available: https://www.mt.com/ca/en/home/products/Transport_and_Logistics_Solutions/Cargoscan_pallet_dimensioning/in-motion-dimensioning-weighing/CSN210.html. [Accessed 18 06 2018].

[7] W.-Q. Shu, "Dynamic weighing under nonzero initial conditions," *IEEE Transactions on Instrumentation and Measurement,* vol. 42, no. 4, pp. 806 - 811, 1993.

[8] R. Tasaki, T. Yamazaki, H. Ohnishi, M. Kobayashi and S. Kurosu, "Continuous weighing on a multi-stage conveyor belt with fir filter," *Measurement,* vol. 40, no. 7-8, pp. 791-796, 2007.

[9] M. Niedźwiecki and A. Wasilewski, "Application of adaptive filtering to dynamic weighing of vehicles," *Control Engineering Practice,* vol. 4, no. 5, pp. 635-644, 1996.

[10] A. Pawłowski, F. Rodr´ıguez, J. Sánchez-Hermosilla and S. Dormido, "Adaptive weighing system with fast nonstationary filtering and centrifugal force compensation," *IEEE Transactions on Instrumentation and Measurement,* vol. 66, no. 12, pp. 3210-3217, 2017.

[11] T. Ono, K. Kameoka and K. Nakajima, "Studies on dynamic measurement method of mass and weight (Part 1): Dynamic weighing method-A," *Bulletin of JSME,* vol. 22, no. 166, pp. 497-503, 1979.

[12] T. Ono, K. Kameoka and K. Nakajima, "Studies on dynamic measurement method of mass and weight (part 2), dynamic weighing method-b," *Bulletin of Japan Society of Electrical Engineers,* vol. 23, no. 177, pp. 439-445, 1980.

[13] H. Gao and W. Pang, "A high-accuracy dynamic weighing system based on single-idler conveyor belt," *International Conference on Machine Learning and Cybernetics,* vol. 4, no. IEEE, pp. 2483-2487, 2009.

[14] T. Umemoto, M. Kamon and Y. Kagawa, "Improvement of accuracy for continuous mass measurement in checkweighers with an adaptive notch filter," *Transactions of the Society of Instrument and Control Engineers,* vol. 47, no. 10, pp. 477-484, 2011.

[15] P. Pietrzak, M. Meller and M. Niedzwiecki, "Dynamic mass measurement in checkweighers using a discrete time-variant low-pass filter," *Mechanical Systems and Signal Processing,* vol. 48, no. 1-2, pp. 67-76, 2014.

[16] T. Yamazaki, Y. Sakurai, H. Ohnishi, M. Kobayashi and S. Kurosu, "Continuous mass measurement in checkweighers and conveyor belt scales," in *Sice Annual Conference*, SICE, 1999, 2002.

[17] J. Emery, "Simplifying the electronic balance load cell," *Sensors Magazine,* vol. 19, no. 6, 2002.

[18] W. Balachandran, M. Halimic, M. Hodzic, M. Tariq, Y. Enab and F. Cecelja, "Optimal digital control and filtering for dynamic weighing systems," in *Instrumentation and Measurement Technology Conference (IMTC)*, Waltham, Mass., 1995.

[19] Y. Yamakawa, T. Yamazaki, J. Tamura and O. Tanaka, "Dynamic behaviors of a checkweigher with electromagnetic force compensation," in *International Measurement Confederation*, Lisbon, 2009.

[20] R. Maier and G. Schmidt, "Integrated digital control and filtering for an electrodynamically compensated weighing cell," *IEEE Transaction on Instrumentation and Measurement,* vol. 38, no. 5, pp. 998-1003, 1989.

[21] C. Diethold and F. Hilbrunner, "Force measurement of low forces in combination with high dead loads by the use of electromagnetic force compensation," *Measurement Science and Technology,* vol. 23, no. 7, p. , 2012.

[22] Y. Yamakawa and T. Yamazaki, "Mathematical model of checkweigher with electromagnetic force balance system," *ACTA IMEKO,* vol. 3, no. 2, pp. 9-13, 2014.

[23] Y. Yamakawa and T. Yamazaki, "Simplified dynamic model for high-speed checkweigher," in *International Journal of Modern Physics: Conference Series*, , 2014.

[24] M. Halimic, W. Balachandran, M. Hodzic and F. Cecelja, "Performane improvement of dynamic weighing systems using linear quadratic gaussian controller," in *Instrumentation and Measurement Technology Conference (IMTC)*, , 2003.

[25] Wipotec GmbH, "Weighing Principle," , . [Online]. Available: https://www.wipotec-wt.com/en/company/weighing-principle/. [Accessed 06 07 2018].

[26] M. Tariq, W. Balachandran and S. Song, "Checkweigher modeling using dynamical subsystems," in *Industry Applications Conference, 1995. Thirtieth IAS Annual Meeting, IAS '95., Conference Record of the 1995 IEEE*, Orlando, FL, USA, 1995.

[27] M. Halimic and W. Balachandran, "Kalman filter for dynamic weighing system," in *Industrial Electronics, 1995. ISIE '95., Proceedings of the IEEE International Symposium on*, Athens, Greece, 1995.

[28] M. Halimic, A. Halimic, S. Zugail and Z. Huneiti, "Intelligent signal processing for electro-mechanical systems," in *Proceeding of the 5th International Symposium on Mechatronics and its Applications (ISMA08)*, Amman, Jordan, 2008.

[29] B. Maassarani, "Dynamic Weighing of Non-Singulated Objects Using a Grid of Decoupled Platforms," University of Waterloo, Waterloo, Canada, 2016.

[30] G. Boschetti, R. Caracciolo, D. Richiedei and A. Trevisani, "Model-based dynamic compensation of load cell response in weighing machines affected by environmental vibrations," *Mechanical Systems and Signal Processing*, vol. 34, no. 1-2, pp. 116-130, 2013.

[31] K. J. Astrom and B. Wittenmark, Adaptive Control, 2 ed., Boston, MA: Addison-Wesley, 1995, p. 734.

Appendix

On the following page are mechanical drawings that show the dimensions and features of the aluminum components that are assembled to form the housing of the conveyor module. Following the mechanical drawings is a wiring diagram of the motor system.

Top flat piece:

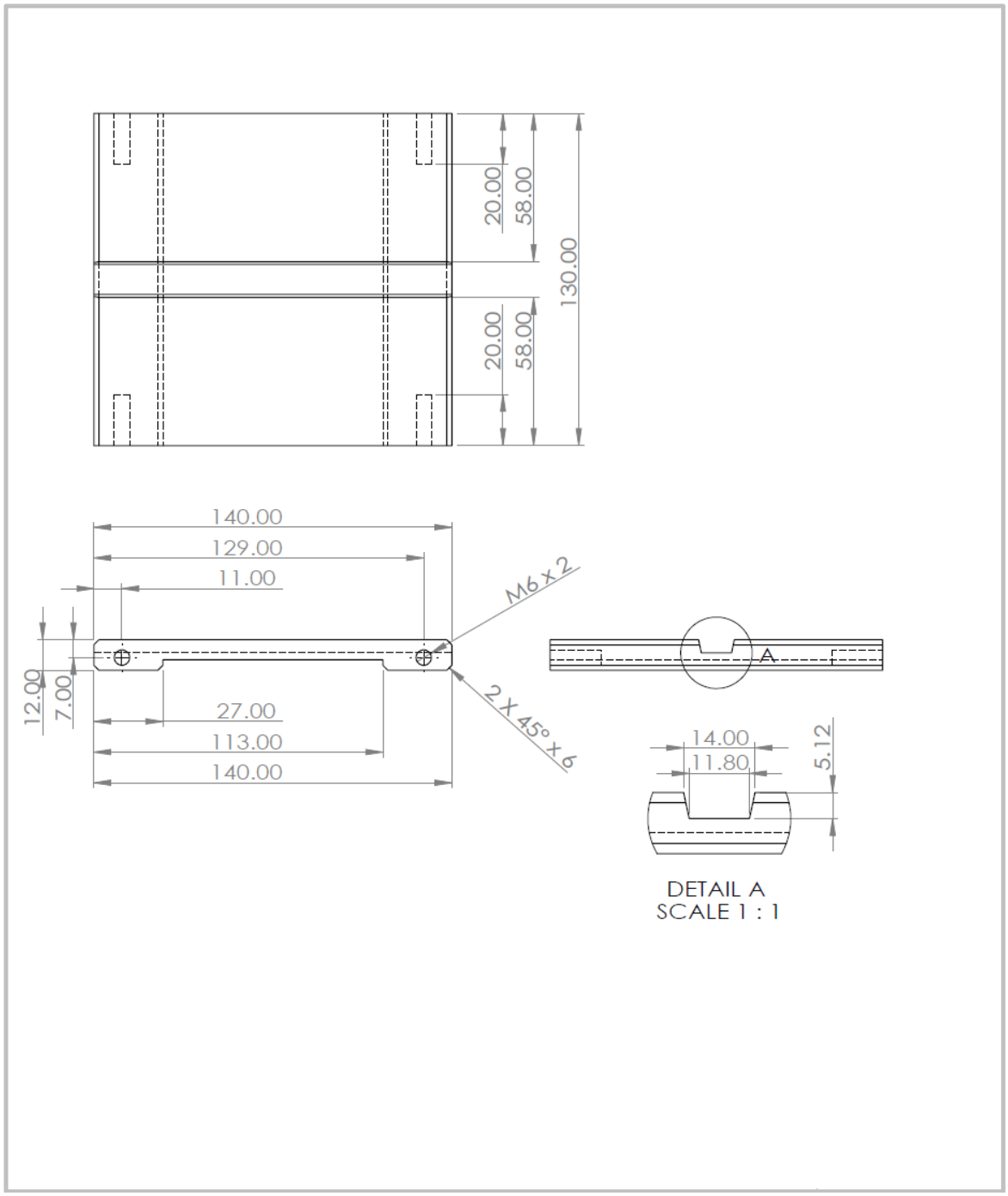

Bottom adjoining pieces:

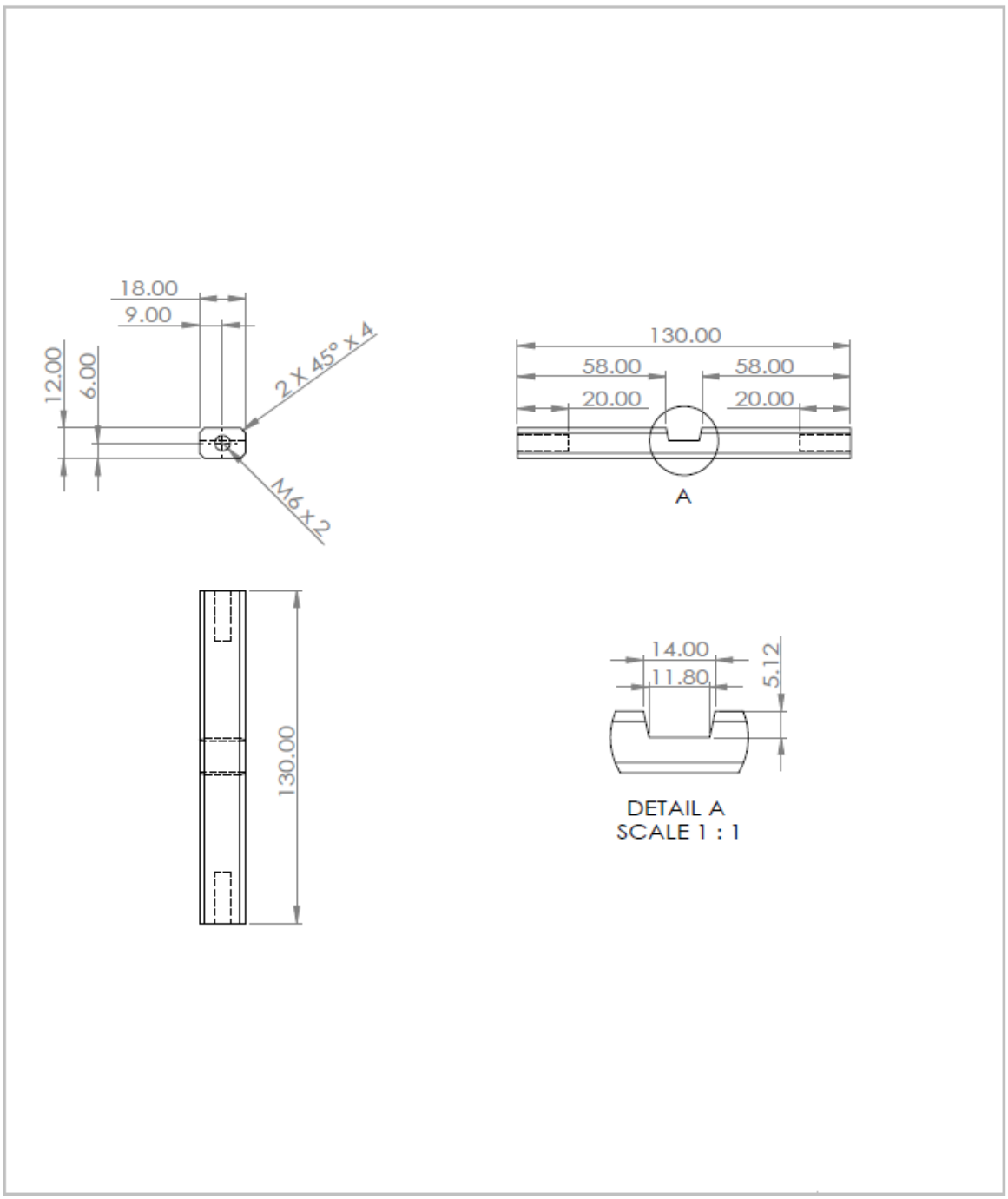

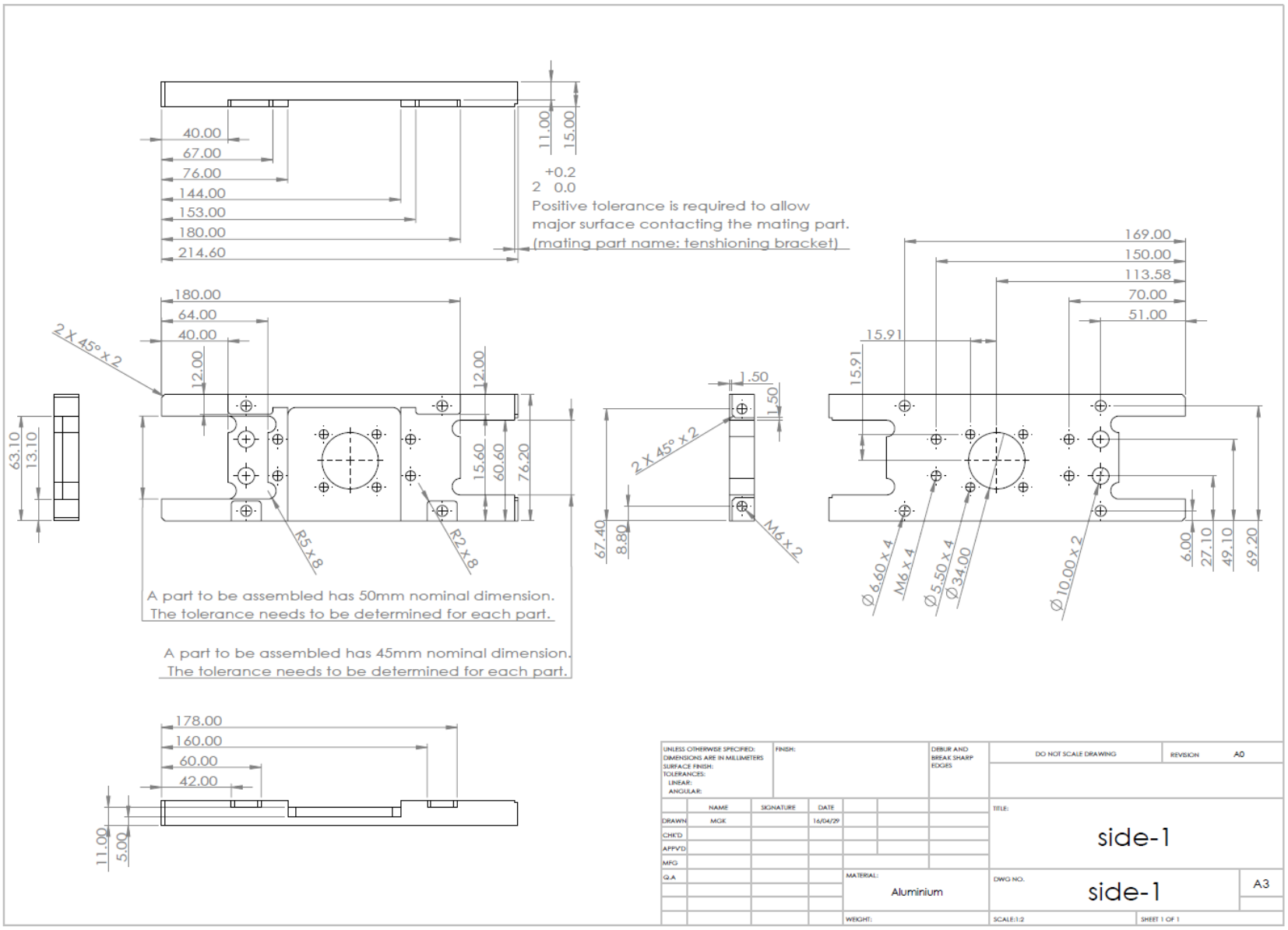
40.00
67.00
76.00
144.00
153.00
180.00
214.60
11.00
15.00
+0.2
2 0.0
Positive tolerance is required to allow
major surface contacting the mating part.
(mating part name: tenshioning bracket)
180.00
64.00
40.00
2 X 45° x 2
12.00
12.00
63.10
13.10
15.60
60.60
76.20
R5 x 8
R2 x 8
A part to be assembled has 50mm nominal dimension.
The tolerance needs to be determined for each part.
A part to be assembled has 45mm nominal dimension.
The tolerance needs to be determined for each part.
1.50
1.50
2 X 45° x 2
67.40
8.80
M6 x 2
169.00
150.00
113.58
70.00
51.00
15.91
15.91
Ø6.60 x 4
M6 x 4
Ø5.50 x 4
Ø34.00
Ø10.00 x 2
6.00
27.10
49.10
69.20
178.00
160.00
60.00
42.00
11.00
5.00
UNLESS OTHERWISE SPECIFIED:
DIMENSIONS ARE IN MILLIMETERS
SURFACE FINISH:
TOLERANCES:
LINEAR:
ANGULAR:
FINISH:
DEBUR AND
BREAK SHARP
EDGES
DO NOT SCALE DRAWING
REVISION
A0
NAME
SIGNATURE
DATE
DRAWN
MGK
16/04/29
CHK'D
APPV'D
MFG
Q.A
MATERIAL:
Aluminium
WEIGHT:
TITLE:
side-1
DWG NO.
side-1
A3
SCALE:1:2
SHEET 1 OF 1

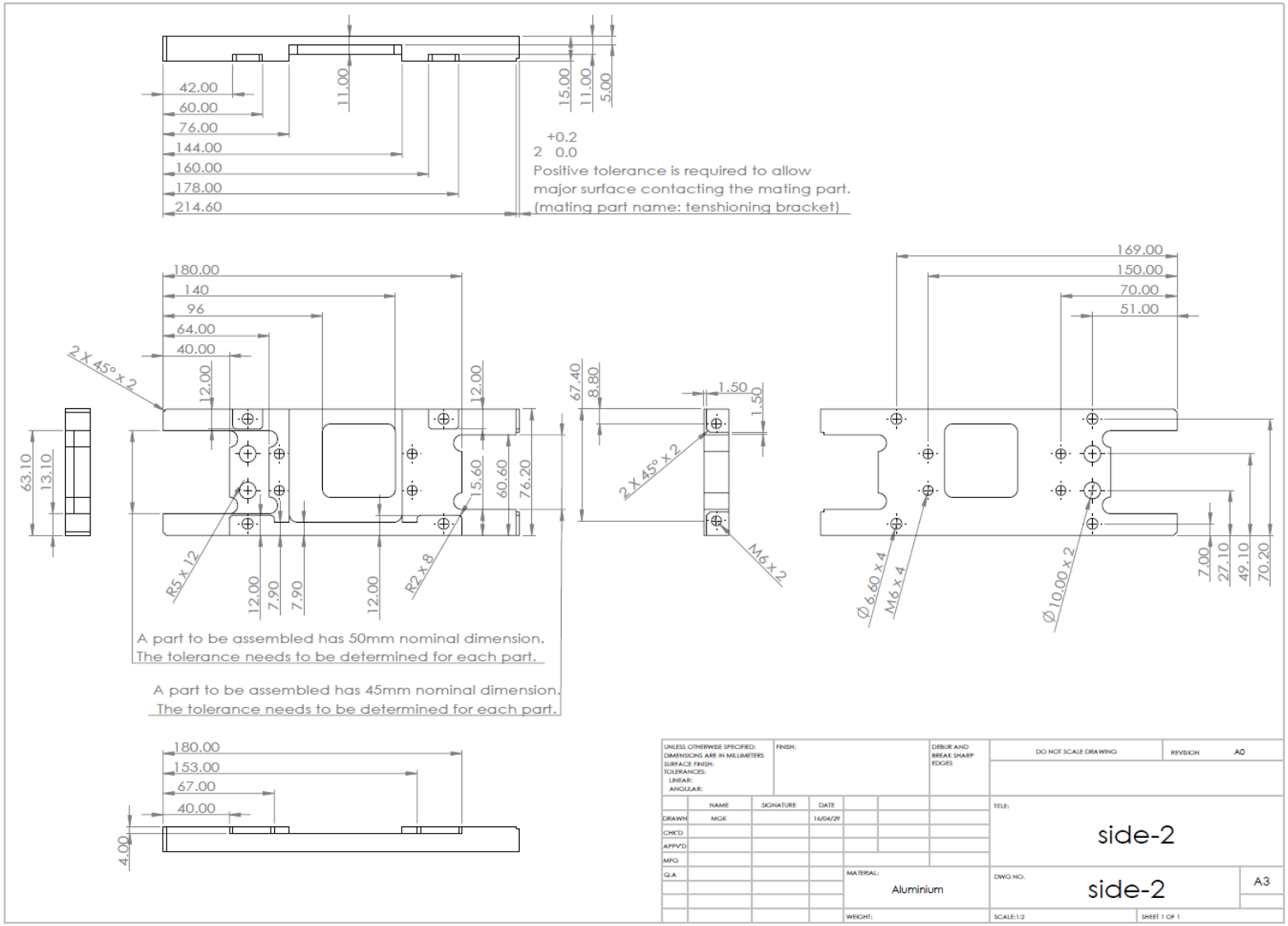
42.00
60.00
76.00
144.00
160.00
178.00
214.60
11.00
15.00
11.00
5.00
+0.2
2 0.0
Positive tolerance is required to allow
major surface contacting the mating part.
(mating part name: tenshioning bracket)
180.00
140
96
64.00
40.00
2 X 45° x 2
12.00
12.00
63.10
13.10
15.60
60.60
76.20
R5 x 12
12.00
7.90
7.90
12.00
R2 x 8
67.40
8.80
1.50
1.50
2 X 45° x 2
M6 x 2
169.00
150.00
70.00
51.00
Ø6.60 x 4
M6 x 4
Ø10.00 x 2
7.00
27.10
49.10
70.20
A part to be assembled has 50mm nominal dimension.
The tolerance needs to be determined for each part.
A part to be assembled has 45mm nominal dimension.
The tolerance needs to be determined for each part.
180.00
153.00
67.00
40.00
4.00
UNLESS OTHERWISE SPECIFIED:
DIMENSIONS ARE IN MILLIMETERS
SURFACE FINISH:
TOLERANCES:
LINEAR:
ANGULAR:
FINISH:
DEBUR AND BREAK SHARP EDGES
DO NOT SCALE DRAWING
REVISION A0
NAME SIGNATURE DATE
DRAWN MGK 16/04/29
CHK'D
APPV'D
MFG
Q.A
MATERIAL: Aluminium
WEIGHT:
TITLE: side-2
DWG NO. side-2
A3
SCALE:1:2
SHEET 1 OF 1

Mounting bar (upper):

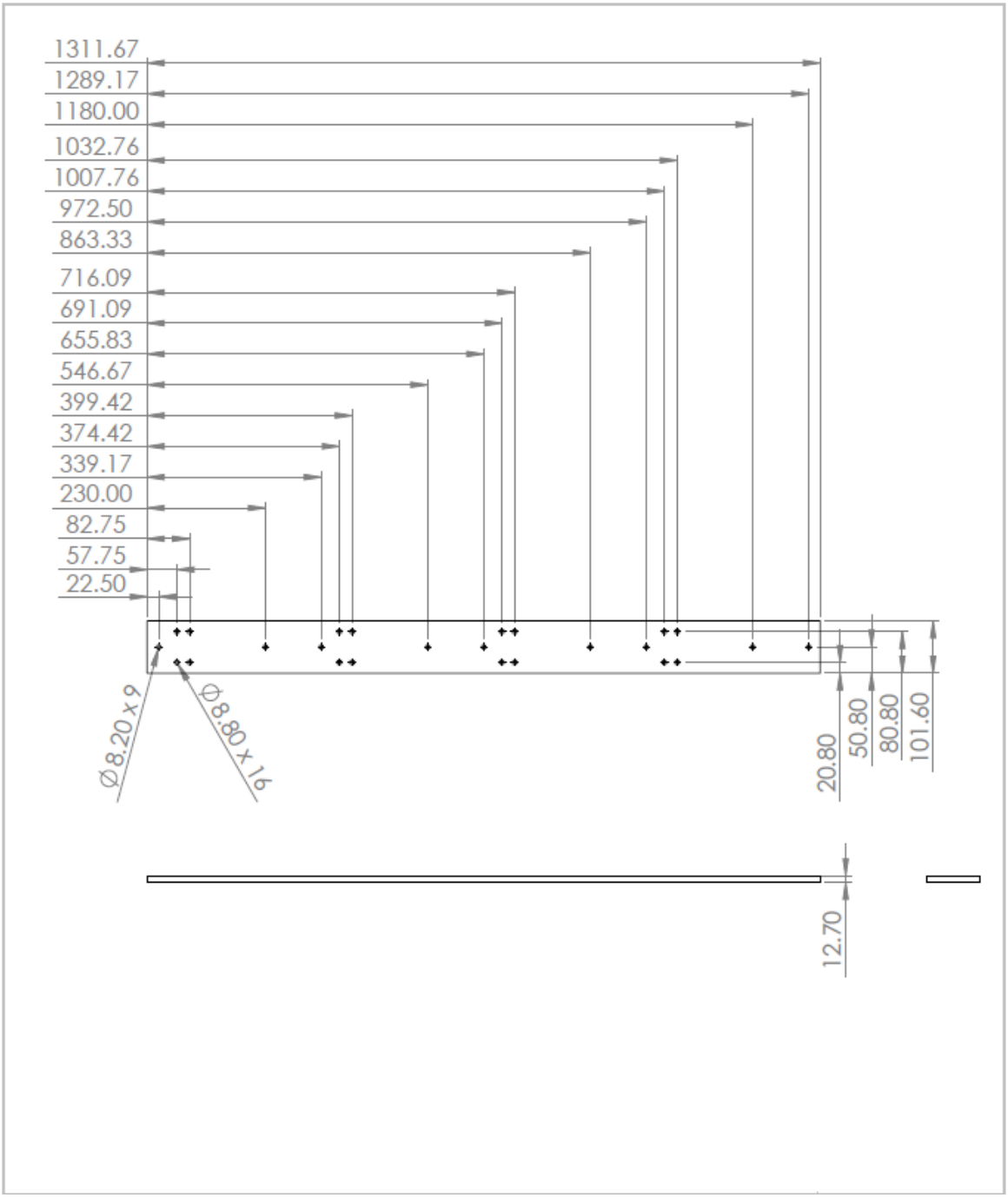

Mounting bar (lower):

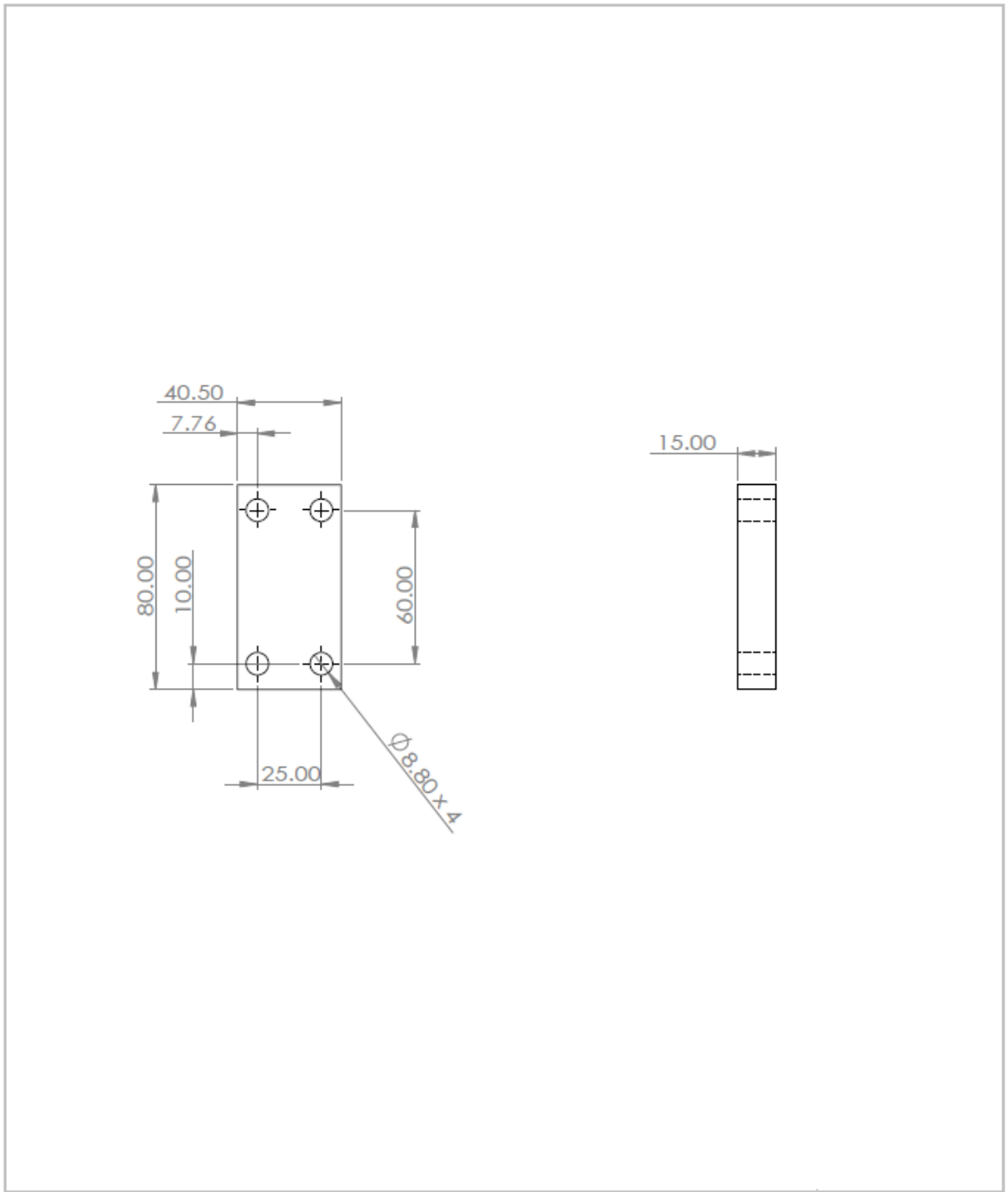

Belt tensioning C-piece:

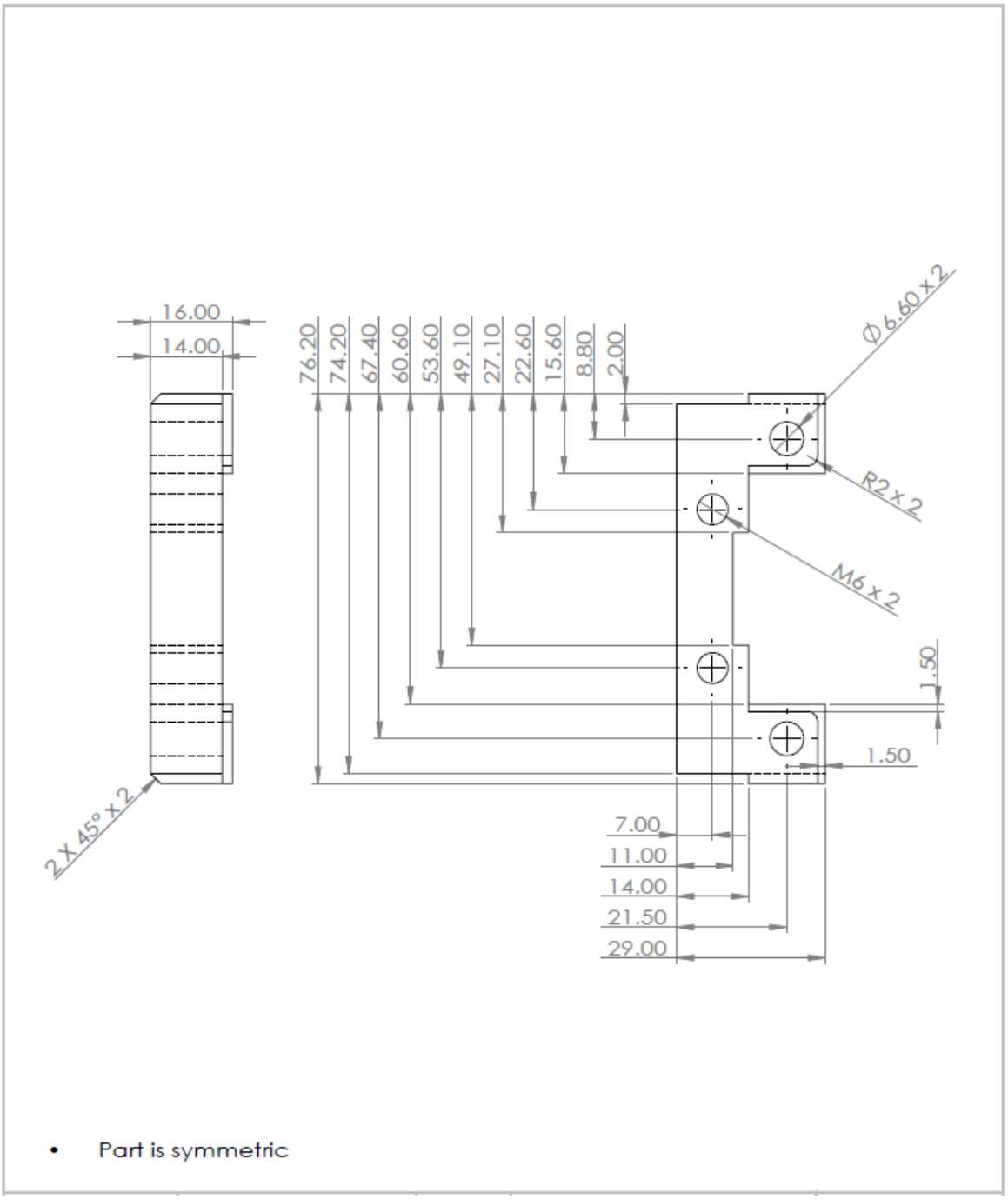

Bottom mounting piece:

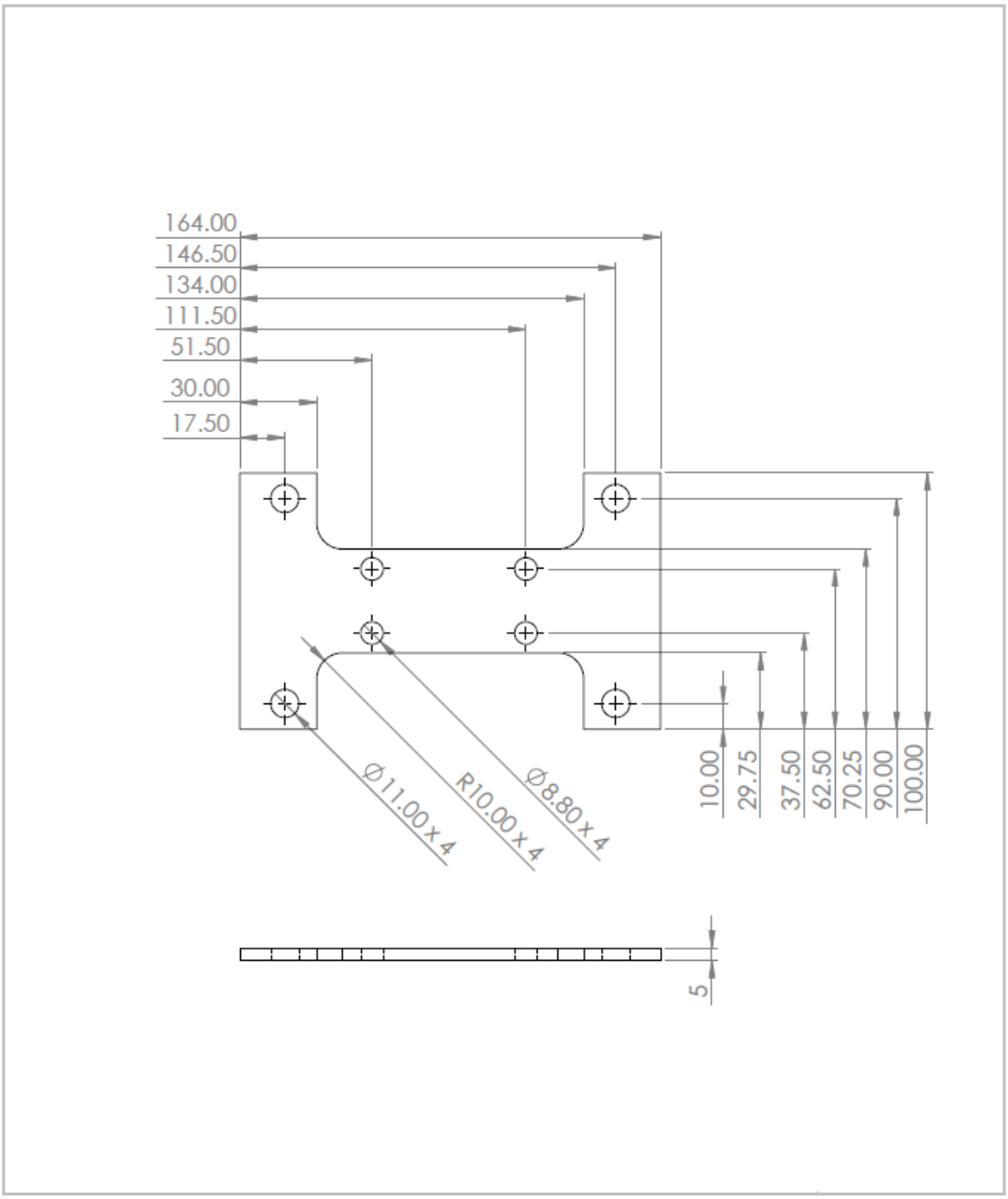

L-brackets:

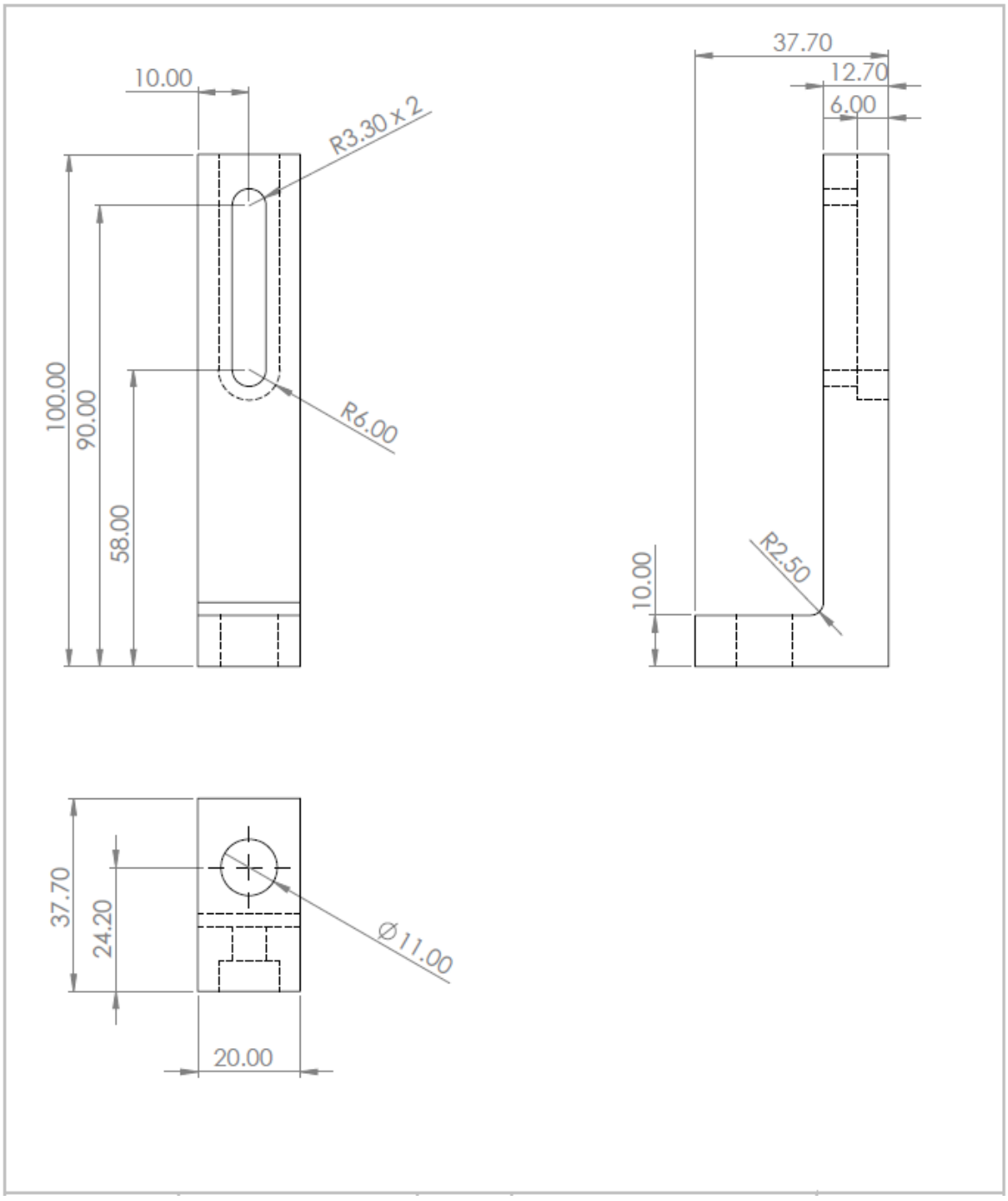
10.00
R3.30 x 2
100.00
90.00
58.00
R6.00
37.70
12.70
6.00
10.00
R2.50
37.70
24.20
Ø11.00
20.00

Shield (thick):

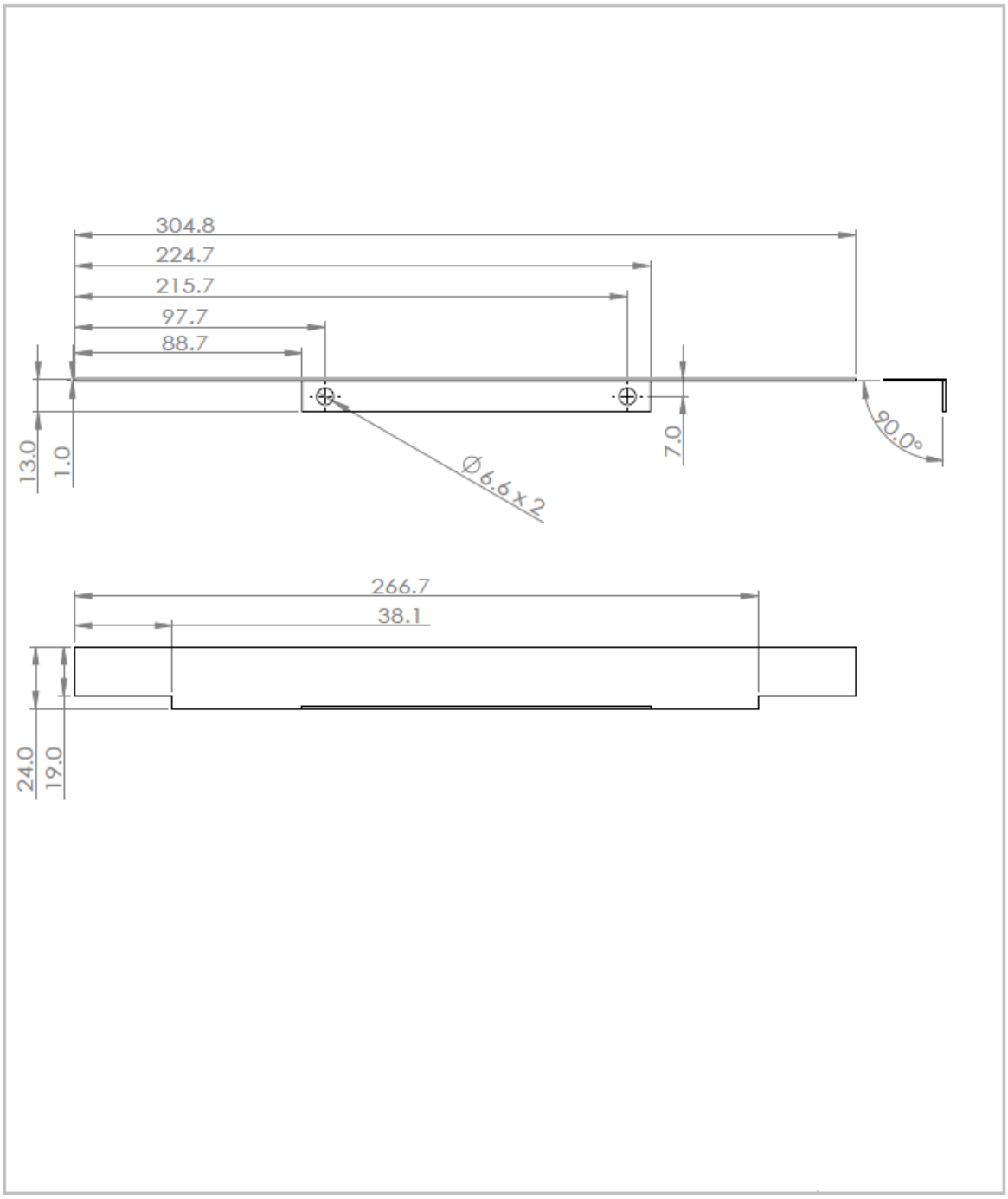

Shield (thin):

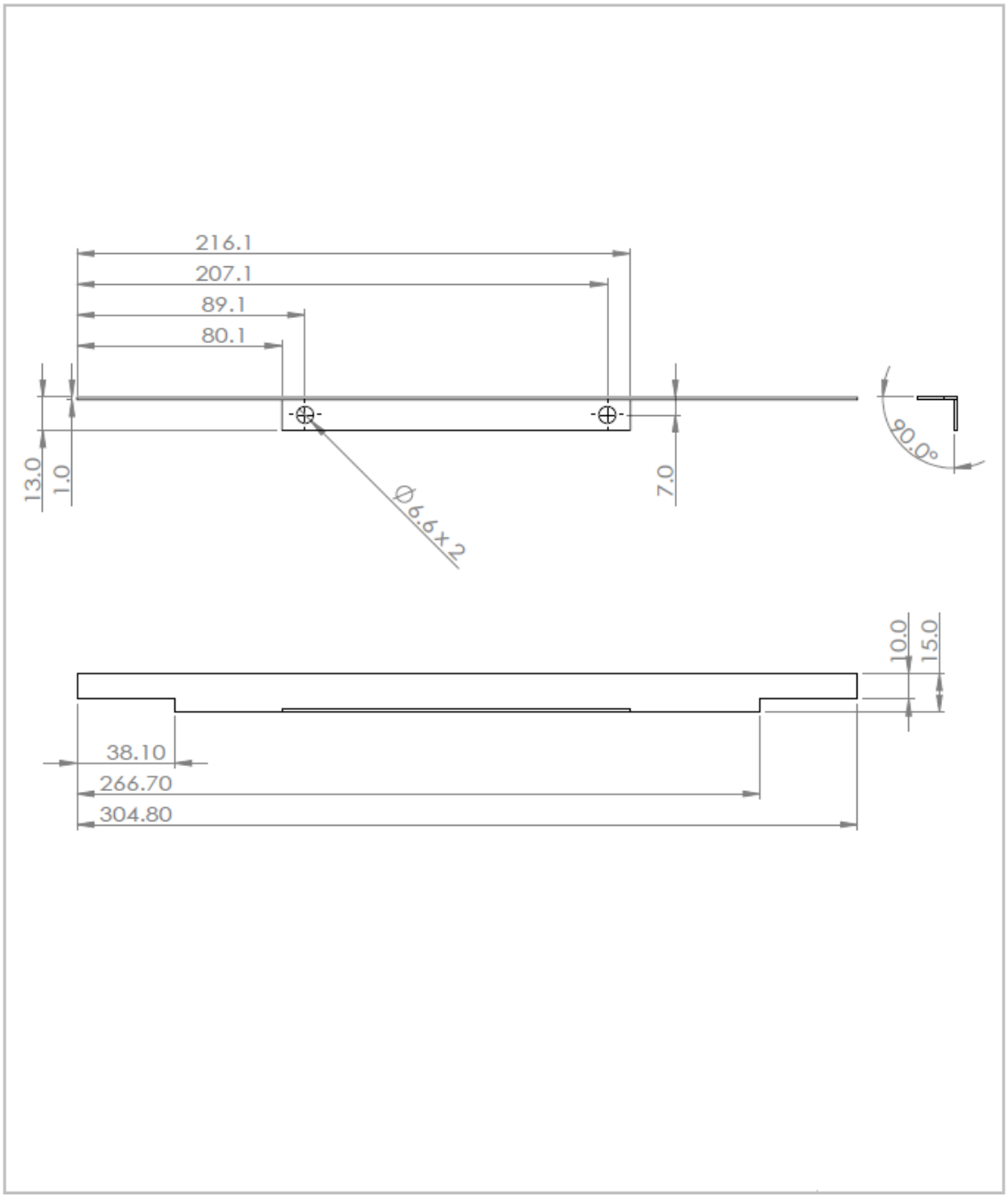

ENC

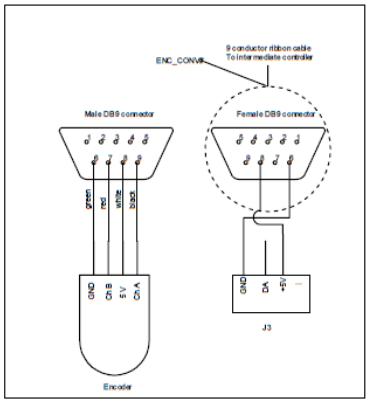
9 conductor ribbon cable
To intermediate controller
ENC_CONV#
Male DB9 connector
Female DB9 connector
green
red
white
black
GND
Ch B
5 V
Ch A
GND
DA
+5V
J3
Encoder

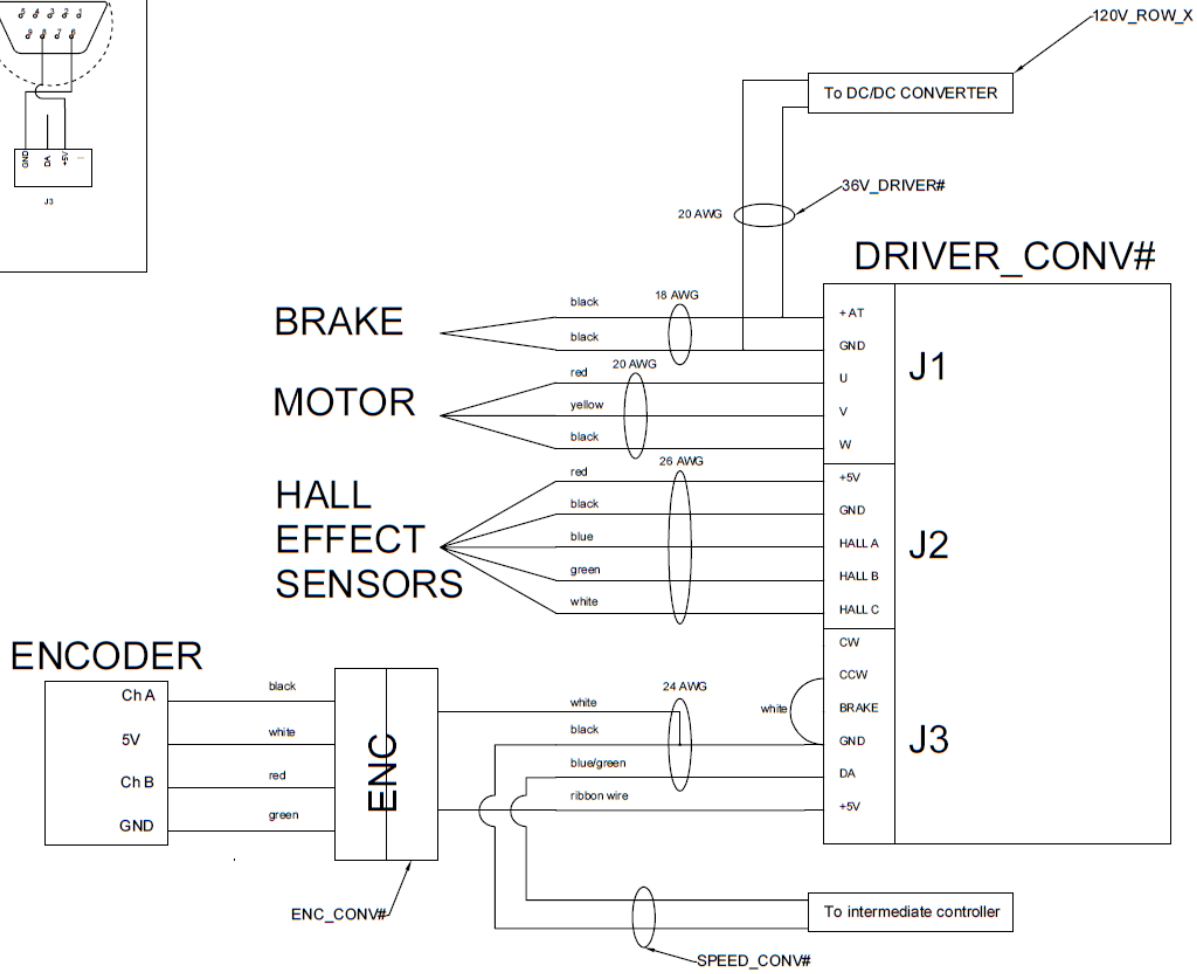
120V_ROW_X
To DC/DC CONVERTER
36V_DRIVER#
20 AWG
DRIVER_CONV#
BRAKE
black
black
18 AWG
MOTOR
red
yellow
black
20 AWG
HALL
EFFECT
SENSORS
red
black
blue
green
white
26 AWG
+ AT
GND
U
V
W
J1
+5V
GND
HALL A
HALL B
HALL C
J2
CW
CCW
BRAKE
GND
DA
+5V
J3
ENCODER
Ch A
5V
Ch B
GND
black
white
red
green
ENC
white
black
blue/green
ribbon wire
24 AWG
white
ENC_CONV#
To intermediate controller
SPEED_CONV#